USE OF A NOVEL MAGNETIC RESONANCE IMAGING BASED MODELING TECHNIQUE TO INVESTIGATE DIFFERENCES IN TIBIOFEMORAL ARTICULAR CARTILAGE CONTACT AREA IN SUBJECTS WITH MODERATE KNEE OSTEOARTHRITIS

by

Christopher E. Henderson

A thesis submitted to the Faculty of the University of Delaware in partial fulfillment of the requirements for the degree of Master of Science in Mechanical Engineering

Fall 2009

USE OF A NOVEL MAGNETIC RESONANCE IMAGING BASED MODELING TECHNIQUE TO INVESTIGATE DIFFERENCES IN TIBIOFEMORAL ARTICULAR CARTILAGE CONTACT AREA IN SUBJECTS WITH MODERATE KNEE OSTEOARTHRITIS

by
Christopher E. Henderson

Approved: _____
Jill S. Higginson, Ph.D.
Professor in charge of thesis on behalf of the Advisory Committee

Approved: _____
Anette M. Karlsson, Ph.D.
Chair of the Department of Mechanical Engineering

Approved: _____
Michael J. Chajes, Ph.D.
Dean of the College of Engineering

Approved: _____
Debra Hess Norris, M.S.
Vice Provost for Graduate and Professional Education

ACKNOWLEDGMENTS

I would like to thank my advisor, Dr. Jill S. Higginson, for her unwavering support through this project. I would also like to thank Dr. Peter Barrance and Dr. Liyun Wang for serving as committee members and offering insightful feedback throughout this project. Dr. Peter Barrance deserves an extended thank you for developing the modeling method used in this project, as well as patiently answering every last one of my questions about it.

TABLE OF CONTENTS

LIST OF TABLES vii
LIST OF FIGURES viii
LIST OF ABBREVIATIONS ix
ABSTRACT x

Chapter
1 INTRODUCTION AND BACKGROUND 1

1.1 Knee joint anatomy and physiology 1
1.2 Background 3

1.2.1 Importance of investigating knee OA 4
1.2.2 Differences between healthy and OA joints 4
1.2.3 Initiation and progression of knee OA 5
1.2.4 Treatments 6
1.2.5 Classifications 6
1.2.6 Risk factors 7
1.2.7 Role of mechanical stress in knee OA progression 8
1.2.8 *In vitro* contact area studies in knee OA 8
1.2.9 *In vivo* medical imaging techniques 10

1.3 Motivation for using MRI 11

1.3.1 The MRI technique 11
1.3.2 Previous MRI based non-contact area studies of the knee joint 12
1.3.3 Previous MRI based contact area studies of the knee joint 13
1.3.4 General limitations to previous MRI based contact area investigations 13

1.4 Specific aims 14

1.4.1 Aim 1: Implement and establish confidence in point cloud modeling method's ability to estimate articular cartilage contact area 15

1.4.2 Aim 2: Evaluate relationship between cartilage contact area and knee flexion in subjects with moderate knee OA and healthy, age matched controls 15

1.5 References 16

2 METHODS 22

2.1 Introduction 22
2.2 Subjects 22
2.3 Data collection process 23
2.4 Excluded data 26
2.5 Image preparation 26
2.6 Digitization process and coordinate system assignment 27
2.7 Generation of reference knee joint model and application to other scans…… 28
2.8 Contact area determination 29
2.9 Normalization of the data 29
2.10 Conclusions 31
2.11 References 32

3 AIM 1: IMPLEMENT AND ESTABLISH CONFIDENCE IN POINT CLOUD MODELING METHOD'S ABILITY TO ESTIMATE ARTICULAR CARTILAGE CONTACT AREA 33

3.1 Introduction and background 33
3.2 Methods 35

3.2.1 Solution uniqueness 36
3.2.2 Method sensitivity 36
3.2.3 Intra-observer reliability 37

3.3 Results 37

3.3.1 Solution uniqueness 37
3.3.2 Method sensitivity 37
3.3.3 Intra-observer reliability 38

3.4 Discussion 40

3.4.1 Solution uniqueness 40
3.4.2 Method sensitivity 41

3.4.3 Intra-observer reliability 41

3.5 Conclusions 42
3.6 References 43

4 AIM 2: EVALUATE RELATIONSHIP BETWEEN CARTILAGE CONTACT AREA AND KNEE FLEXION IN SUBJECTS WITH MODERATE KNEE OA AND HEALTHY, AGE MATCHED CONTROLS 45

4.1 Introduction and background 45
4.2 Methods 47

4.2.1 Subjects…. 47
4.2.2 Data acquisition 47
4.2.3 Data processing 48
4.2.4 Data analysis 49

4.3 Results 49
4.4 Discussion 53
4.5 Conclusions 56
4.6 References 57

5 CONCLUSIONS AND FUTURE WORK 59

REFERENCES 61

LIST OF TABLES

Table 1.1 Cadaveric studies of medial and lateral compartment tibiofemoral contact area in healthy subjects 9

Table 1.2 MRI based studies of tibiofemoral contact area in healthy subjects..... 13

Table 3.1 Subject characteristics 35

Table 3.2 Results of evaluation of method sensitivity..... 38

Table 4.1 Group characteristics 50

Table 4.2 Estimates of group articular cartilage contact area generated from linear regression lines 53

LIST OF FIGURES

Figure 1.1 Knee joint anatomy 2

Figure 2.1 Schematic of custom knee positioning device showing subject positioning 25

Figure 2.2 Superior surface of tibial plateau with anterior-posterior and medial-lateral axes drawn 30

Figure 3.1 Correlation of two tracings of same MRI set after 30 days had passed 39

Figure 3.2 Articular cartilage contact area estimate at partial weightbearing 40

Figure 4.1 Articular cartilage contact area in the medial compartment of the tibiofemoral joint plotted against knee flexion angle in moderate knee OA subjects and healthy controls with corresponding regression lines 51

Figure 4.2 Normalized articular cartilage contact area in the medial compartment of the tibiofemoral joint in healthy controls and OA subjects 52

LIST OF ABBREVIATIONS

ACL = anterior cruciate ligament

BMI = body mass index

CT = computed tomography

CV = coefficient of variation

FEA = finite element analysis

JSN = joint space narrowing

KL = Kellgren and Lawrence

LC = lateral compartment

MC = medial compartment

MRI = magnetic resonance imaging

OA = osteoarthritis

TrICP = trimmed iterative closest point algorithm

ABSTRACT

Knee osteoarthritis (OA) detrimentally impacts the lives of millions of older Americans through pain and decreased functional ability. Unfortunately, the pathomechanics and associated changes that OA patients experience are not well understood. Mechanical stress in the knee joint may play an essential role in OA; however existing literature in this area is limited. **Purpose:** The purpose of this study was two-fold. First, we wanted to evaluate an existing magnetic resonance imaging (MRI) based modeling method's estimation of articular cartilage contact area *in vivo*. Secondly, we wanted to apply this method to a cohort of subjects with moderate knee OA and compare their medial compartment articular cartilage contact area estimates with healthy, age matched controls. **Methods:** In order to establish confidence in the modeling method's ability to estimate articular cartilage contact area, imaging data on a single, healthy subject were collected and compared to existing contact area estimates in the literature. Intra-observer reliability and sensitivity studies were also performed in an attempt to further establish confidence in the method. In the second half of this study, MRIs of the knee at 0°, 15°, and 30° flexion were collected during partial-weightbearing in subjects with moderate knee OA (n = 11) and healthy, age matched controls (n = 11). Articular cartilage contact area estimates were normalized to an approximation of the surface area of the tibial plateau in order to account for joint size differences between subjects. The relationship between medial compartment articular cartilage contact area and knee flexion was investigated in each group. **Results:** The single healthy subject was found to have articular cartilage contact area

estimates similar to those reported in the literature. The method was found to be sensitive to changes in the cartilage tracings on the peripheries of the compartment and demonstrated an intra-observer reliability of 0.95 when assessed using Pearson's correlation coefficient. In the second half of the study, medial compartment articular cartilage contact area in the healthy controls was found to be significantly correlated with knee flexion angle ($p \leq 0.01$), while no such correlation was found in the moderate OA subjects ($p = 0.34$). Linear regression analysis found that the moderate knee OA subjects had higher articular cartilage contact areas than their healthy, control counterparts across all flexion angles considered. **Conclusions:** Confidence was established in the MRI based knee modeling method's ability to estimate articular cartilage contact area through a series of assessments and comparison with existing literature on healthy subjects. Healthy subjects were found to have a significant correlation between medial compartment articular cartilage contact area and knee flexion, which agreed with the literature. The moderate OA subjects did not show the same relationship between medial compartment articular cartilage contact area and knee flexion. Regression analysis found that they had higher medial compartment articular cartilage contact area estimates in all instances when compared with healthy controls. Increased contact area may be a biomechanical adaptation in response to OA in order to decrease the mechanical stress applied across the painful joint.

Chapter 1

INTRODUCTION AND BACKGROUND

1.1 Knee joint anatomy and physiology

The knee is an important weightbearing joint that provides support for the body as well as serving essential functions during gait. During gait, it is not uncommon for the knee to be loaded several times the weight of the person (53). The knee joint complex is comprised of three bones: the patella, tibia, and femur. These three bones articulate the three joints of the knee: the patellofemoral and medial and lateral tibiofemoral joints. The motion of the patellofemoral joint is caused by the sliding of the patella along the patellar groove of the femur during flexion and extension. Articular cartilage on both the femur and patella allow this sliding motion to occur with very low friction. The patellofemoral joint is tensioned by the quadriceps and the patellar tendon. The quadriceps muscle group inserts into the patella via the patellar ligament and the patella inserts into the proximal anterior tibia via the patellar tendon. The medial and lateral tibiofemoral joints are the result of the epicondyles of the femur articulating with the proximal tibia on the tibial plateau. Hyaline cartilage covers the articulating surfaces of both bones and fibrocartilage in the form of a medial and lateral meniscus surround the contact surfaces and serve an important role in shock absorption. There are also four ligaments that span the tibiofemoral joints to assist in stability and control the motion of the joint. The anterior and posterior cruciate ligaments restrict movement in the sagittal plane, while

the medial and lateral collateral ligaments perform similarly in the frontal plane. The knee joint is characterized as a modified hinge joint as it primarily allows flexion and extension, but also allows for some internal and external rotation during non-weightbearing when in a flexed position (28) (Figure 1.1).

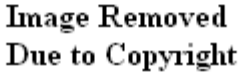

Figure 1.1 Knee joint anatomy (40)

The articular cartilage that covers the surfaces of the knee joints is primarily comprised of an extracellular matrix. The specific type of collagen and proteoglycans that comprise the extracellular matrix differentiate articular cartilage

from other types of cartilage. Healthy cartilage has four zones or layers: superficial, middle, deep, and calcified cartilage. The first three layers do not have well defined boundaries and are quantified based on the orientations of their collagen fibers while the calcified cartilage layer is separated from the rest by the tidemark. The superficial layer has fibers that are oriented tangentially in order to best resist the shear forces generated when the bones slide across each other. The middle layer, which makes up 40-60% of the total cartilage thickness, has its fibers randomly oriented, while the deep layer has its fibers oriented perpendicular to the articular surface in order to best resist normal load and prevent the cartilage from peeling off the bone. The calcified cartilage is the transition between bone and cartilage and has a primary function of anchoring the cartilage to the bone (36).

The porous nature of articular cartilage allows the synovial fluid secreted by the joint capsule to lubricate the joint. Synovial fluid is a highly viscous liquid that also aids in supplementing the cartilage stiffness during loading. The increased stiffness is a result of the high water content in the synovial fluid and translates to a high level of incompressibility for the synovial fluid which is used advantageously by the cartilage during loading.

1.2 Background

OA is a degenerative joint disease and is the most common form of arthritis (4). It is defined as a group of signs and symptoms that suggest joint deterioration. Articular cartilage is usually the primary focus of OA; however changes in the subchondral bone and meniscus also must be considered (2). Clinical diagnosis of OA is made on the basis of joint symptoms and radiographic evidence (22) with the primary symptoms of OA being pain and instability (23).

1.2.1 Importance of investigating knee OA

Tibiofemoral or knee OA is highly burdensome on the US population. It has been cited as one of the top five leading causes of disability in the elderly (4) and costs the US economy more than $60 billion per year (15). Approximately 11% of people greater than 60 years of age have symptomatic knee OA (15,22) and those that choose to go to the hospital for treatment have an average stay of five days and a cost of $18,000 (4). Although knee OA has been studied extensively over the past several decades, important questions still persist. It is not known what initiates OA, what causes the disease to progress, nor specifically why OA is painful. Pain is difficult to quantify in people and is restricted to subjective responses on surveys. Important variables such as pain, joint use, and joint degeneration are difficult to study in animal models (15). Physiologically relevant joint use is difficult to model in animals as well. Almost all animals used in research studies are quadrupeds and all animal models have anatomically different joints which further limit implications of the studies. Cartilage is aneural and although pain fibers have been observed within the synovium, near ligament insertions, in bones, muscles and outer third of the meniscus (23), it is not well understood why people with similar radiographic symptoms have differing levels of pain and disability (4).

1.2.2 Differences between healthy and OA joints

Andriacchi et al. (7) hypothesized that OA represents an inability on the part of the cartilage cells to maintain homeostasis. They concede that there is an expected decline in the efficacy to which the cells are able to maintain homeostasis with increasing age; however OA demonstrates several biological changes that are not seen in healthy aging joints. Changes in water content of cartilage can also serve as a

precursor to OA development. Aged healthy cartilage should have about the same water content as young healthy cartilage, however as OA develops, water content has been shown to increase (4).

1.2.3 Initiation and progression of knee OA

Investigators have identified that OA needs to be studied in two distinct phases: initiation and progression (7). Studies have shown that the risk factors for the initiation of OA are different than those for progression (37). The initiation phase is usually characterized by kinematic changes that shift loadbearing to areas of cartilage not usually expected to handle loadbearing and as a result are unable to accommodate the loads (7). Other investigations have shown that changes in subchondral bone are associated with OA initiation, but have been unable to conclusively demonstrate if the subchondral bone changes cause the breakdown of articular cartilage or whether the breakdown of articular cartilage results in subchondral bone changes (8).

The progression phase begins after the cartilage begins to break down and causes of progression are not well understood. Elucidating risk factors for progression of knee OA has been difficult because studies have shown that OA progression may cease for years at a time (14) and because the literature as a whole lacks a gold standard of what qualifies as progression of the pathology (37). In spite of these limitations, the results of a study by Andriacchi et al. (7) suggests that OA progression was expedited by increased loading and found that some subjects were able to adopt strategies that decreased the load at the joint and reduced the rate of progression.

1.2.4 Treatments

The lack of a foundation of understanding of the OA pathology makes effective medical treatment difficult. Strengthening of the surrounding muscles, anti-inflammatory drugs, bracing, and surgery are all prescribed depending on the severity of the pathology and the level of pain and discomfort that the patient is experiencing (5). Studies have shown that exercising is occasionally effective, but sometimes has a detrimental effect (23). Anti-inflammatory drugs have been shown to decrease pain, but increase knee adductor moments (14) which in turn increase the likeliness of progression (37). Two types of braces are sometimes prescribed in an attempt to limit OA progression. An "unloader" brace is used to divert loading away from the afflicted side of the knee, while a "support" brace is used to decrease the load on the entire knee. The American Academy of Orthopaedic Surgeons suggests that arthroscopy with debridement is the first surgical procedure considered, although tibial osteotomies are sometimes used to improve frontal plane knee alignment. A major limitation to the tibial osteotomy is that it almost always leads to total knee arthroplasty (5).

1.2.5 Classifications

Knee OA is primarily classified into two groups: primary and secondary. Primary or idiopathic knee OA is characterized by the patient having no prior event or disease related to the development of knee OA, while secondary knee OA is defined as OA that develops due to some sort of joint trauma or other disease associated with the development of OA (2). The severity of OA is currently assessed by joint space narrowing (JSN), presence of osteophytes (bone spurs), and patient signs and symptoms. In the case of knee OA, JSN is usually assessed on anterior-posterior radiographs with the knee at full extension or in a semi-flexed position and is usually

measured in the medial compartment (25). Joint space width measures the distance between the femur and tibia at a single point and subtracts it from an expected width in order to calculate JSN (2). Kellgren and Lawrence developed the most common measure of OA progression in 1957. The Kellgren and Lawrence (KL) grade uses JSN in conjunction with other joint abnormalities found on an anterior-posterior radiograph such as osteophytes development to give the joint a score from zero to four. A KL grade of zero indicates a complete absence of OA, while a grade of two indicates a definite presence of OA, but of minimal severity and a grade of four indicates severe OA (32). The major advantage of the KL grading scale is the low cost and quick scoring. However, the KL grade is limited in its assessment of OA because it depends on an experienced radiologist to be properly read. The orientation of the joint can also cause inaccuracies in the measuring of the JSN. As a result of JSN only being measured at a single point, it is only able to provide limited information about the overall changes that the joint is undergoing (6). Quantifying OA progression is complicated even further by studies that have also shown mild to moderate JSN can be caused by meniscal extrusion and not actually cartilage degradation (50). These limitations make it more difficult to properly separate OA subjects into groups in research studies of the pathology (32). Until a better system can be developed, KL grading acts as the standard for assessing OA severity (3).

1.2.6 Risk factors

Although the causation and progression (or lack thereof) of the disease is not well understood, research studies have been able to identify a series of risk factors for knee OA. It has been shown that men are more likely to develop the disease before age 50, but after age 50, females have a greater incidence (22). Obesity has been

reported to be a risk factor for incidence of knee OA, but not progression (39). History of sports participation (17), meniscal damage (11), and high knee adduction moments (37) have all been shown to be risk factors for incidence of knee OA. Despite known correlations between the knee adduction moment and knee alignment, knee alignment has been shown not to be a risk factor for incidence of knee OA (31). High bone density has been shown to be a risk factor for incidence of knee OA, while low bone density has been shown to be a risk factor for progression of knee OA (4).

1.2.7 Role of mechanical stress in knee OA progression

Previous investigators have suggested that OA represents a failure of the body to perform necessary cellular maintenance due to excessive mechanical stress (14). Mechanical stress is directly proportional to the load applied and inversely proportional to the area over which the load is distributed. Through use of an instrumented knee prosthesis, a previous study has linked medial compartment joint loading with the knee adduction moment (53). The knee adduction moment has previously been identified to correlate with OA progression (37). The results from these investigations support the loading component of the mechanical stress hypothesis; however the area on which the load is distributed, or contact area, has not fully been investigated in the knee OA population.

1.2.8 *In vitro* contact area studies in knee OA

Studying contact area in the knee is not a novel idea. In the past, researchers have used cadavers and pressure sensitive film in an attempt to measure contact area (1,24,33,34). Some have estimated the contact area including the meniscus (1,34), after removing the meniscus (33), and some have reported both (24).

Table 1.1 displays the results of these investigations; however, the usefulness of results from cadaveric knee studies are inherently limited by questions about joint alignment, the high average age of most cadavers, and application of physiologically meaningful loads. The use of pressure sensitive film is also problematic due to the complex three dimensional contours of the tibiofemoral joint. Small folds in the film during loading exaggerate the contact area estimate.

Table 1.1 Cadaveric studies of medial and lateral compartment tibiofemoral contact area in healthy subjects (MC = medial compartment, LC = lateral compartment, ~ denotes that value was interpolated from figure)

Investigators	# Subjects	Contact with Meniscus Included?	Load Applied (N)	0° flexion (mm^2)		15° flexion (mm^2)		30° flexion (mm^2)	
				MC	LC	MC	LC	MC	LC
Kettelkamp (33)	14	no	29 - 79	~480	~300	~400	~270	~380	~250
Fukabayashi (24)	6	no	500	240	160				
Fukabayashi (24)	5	yes	500	530	420				
Lee (34)	12	yes	1800	533				477	

Finite element analysis (FEA) of tibiofemoral contact area has also been attempted (19,21,52). The validity of FEA simulations depend on the material properties, accuracy of joint geometry, and orientation and magnitude of forces applied. Generally speaking, material properties of human tissue are difficult to quantify because samples from cadavers are subjected to the same limitations that plague the cadaveric contact area studies. Accurate representations of the bones, cartilage, and other soft tissues are essential to obtain meaningful results and

simplifications such as ignoring the patella (19) would most surely have an effect on the load distribution across the knee. Aside from properly identifying the weight vector to apply across the knee, muscle force vectors also need to be included. A previous study combined musculoskeletal modeling with FEA to estimate contact mechanics (10), but other FEA seem to apply arbitrary estimates of force vectors (19,21,52). FEA is a very promising tool, especially if it could be combined with an imaging technique to generate accurate joint geometry and estimates of muscle force through musculoskeletal simulations, however; to the best knowledge of the researcher, no such study has been conducted on the tibiofemoral joint.

1.2.9 *In vivo* medical imaging techniques

Recently, attention has been paid to visualizing the OA pathology *in vivo*. In vivo imaging presents a unique opportunity to study joint kinematics. A more thorough understanding of joint kinematics is essential for understanding risk factors for initiation and progression of knee OA (41). As previously mentioned, radiographs are central in determining the KL grade of OA progression. The use of radiographs to study OA is limited however. It does not allow for visualization of the cartilage and is highly dependent on patient orientation during imaging. The sensitivity to patient orientation makes it difficult to use radiographs as a means of assessing progression of the pathology. Radiographic assessment of JSN is also susceptible to "pseudo-widening". Pseudo-widening of the knee joint occurs when there is unequal degradation of the medial and lateral compartments. In the case of approximately 20% of knee OA subjects, lateral compartment OA occurs more rapidly than the medial compartment. This causes a pseudo-widening of the medial compartment and underestimating of the severity of the pathology on the medial side (23).

Arthroscopies are also sometimes used to study knee OA. One advantage of arthroscopies is that they provide direction visualization of the cartilage; however they are invasive and provide only semi-quantitative measurements of the cartilage surface (45). Previous studies have also used computed tomography (CT) in conjunction with radiographs to study knee contact kinematics (9). Implications of these results are limited because the method does not allow for visualization of the cartilage and as a result limits data on cartilage to approximations at best.

1.3 Motivation for using MRI

MRI has become a popular imaging tool for knee OA (16,25,46,50) because it allows for direct visualization of the cartilage and other soft tissues. It is considered the best available technique for assessing cartilage morphology and detecting pathology *in vivo* (26). The direct visualization of cartilage is highly desirable for studies of OA progression because it limits the dependence on subject position, a major weakness of radiographic progression studies (50). Another major advantage of MRI is its ability to manipulate tissue contrasts to highlight specific tissues. In the case of knee OA, where cartilage visualization is important, the MRI scan parameters can be manipulated to increase the contrast between the cartilage and surrounding structures and tissues (26).

1.3.1 The MRI technique

Magnetic resonance imaging uses the combination of an extremely strong magnet and radiofrequencies to generate images of polar nuclei. Hydrogen nuclei in the form of water are most important for visualization of soft tissue. The underlying idea is that different tissues, although all containing hydrogen atoms within water

molecules, allow for different levels of mobility for the water molecules. The differing levels of mobility dictate how the tissues are displayed in the image.

1.3.2 Previous MRI based non-contact area studies of the knee joint

Previous investigations have used MRI to study knee kinematics by combining it with dual fluoroscopy to dynamically study the knee *in vivo* (13,18,35). Results from these studies are promising; however, due to limitations in the field of view of the fluoroscopy machines, a single leg lunge is the only motion that has been studied and subjects with knee OA have not been considered. Knee joint centroids, or centers of contact, have also been studied previously (29,41,48,51) in an attempt to better understand knee kinematics. Shefelbine et al. (48) found that healthy controls had contact centroids in both the medial and lateral compartments that were significantly more posterior than subjects with an anterior cruciate ligament deficiency. These results are promising, but to the best of the researcher's knowledge, no study has investigated the knee centroid in OA subjects.

Previous MRI based studies have also focused on cartilage volume (16,25,42,46,50) which is logical as degradation of cartilage is a hallmark of OA. Several investigations found significant differences in cartilage volume between baseline and follow-up (42,46,50), while another did not (25). Studies of volume are limited by focusing on volume as a singular measurement rather than a product of the thickness and surface area (20). A single study focused on cartilage thickness (49), but surface area and more specifically contact area is hypothesized to play a significant role in both initiation and progression of knee OA (14).

1.3.3 Previous MRI based contact area studies of the knee joint

Previous studies have applied MRI in an attempt to quantify contact area *in vivo* (Table 1.2). The recent technological advancement of "open" MRI has made it possible to apply physiologically representative loads to the knee during MRI acquisition. Prior to open MRI, studies were either non-weightbearing (30,38,43) or pseudo-weightbearing (41,48). Pseudo-weightbearing studies used some sort of custom device to apply a load to the bottom of the foot to simulate weightbearing. Based on a careful review of the literature, no full-weightbearing studies have been carried out that quantify tibiofemoral contact area. However one previous study did use full weightbearing to quantify patellofemoral contact area (27).

Table 1.2 MRI based studies of tibiofemoral contact area in healthy subjects. (~ denotes that value was interpolated from figure)

Investigators	# Subjects	Contact with Meniscus Considered?	Load Applied (N)	0° flexion (mm^2)		15° flexion (mm^2)		30° flexion (mm^2)	
				MC	LC	MC	LC	MC	LC
Patel (41)	10	no	133	374	276	~355	~265	~340	~270
Hinterwimmer (30)	12	no	0	487	220			404	299

1.3.4 General limitations to previous MRI based contact area investigations

Previous studies have shown promise in studying knee contact area, but have several limitations. Most previous studies used closed MRIs that were either entirely non-weightbearing or pseudo-weightbearing (12,30,38,41,43,48). Studies commonly employed a Riemann sum technique to estimate contact area by summing the length of contact on each slice and multiplying it by the slice thickness (12,27,41).

This provides an approximation of contact area, but is limited in accuracy by the slice thickness. Most studies also fail to account for the covariate of joint size in their contact area calculations. A large male will have a much larger contact area than a small female, even if they have identical joint geometries. A limited number of previous investigations have applied normalization techniques (12,41) in an attempt to correct for these differences, but most do not (27,30,43,48). Comparing results between studies is also difficult because some studies included meniscal-articular cartilage contact area in their assessment (1,34,48), others do not (30,33,38,41,43) and some calculate both (24). In the interest of assessing mechanical stress in the knee, meniscal contact should only be considered if it has a loadbearing function. Unfortunately, there is disagreement in the literature as to whether it serves in that capacity with some investigators suggesting it has a substantial contribution (48), while other investigators suggest that it has a minimal, if not negligible, contribution (41,43). Contact area has been thoroughly studied *in vivo* in the healthy population (38,41,43) and with pathological populations such as ACL-deficient individuals (48) and patients with patellar subluxation (30); however no *in vivo* MRI based measurements of contact area have been performed in the knee OA population. One previous cadaveric case study was found that studied contact area in knee OA (24); however it had only two subjects.

1.4 Specific aims

Knee OA is both financially costly and physically debilitating, but its underlying mechanism for initiation and progression remains largely unknown. The overall objective of this study is to establish confidence in a knee modeling method's ability to estimate cartilage contact area and use this method to investigate differences

in knee joint contact area in subjects with moderate knee OA and healthy controls. This will be achieved through the following specific aims.

1.4.1 Aim 1: Implement and establish confidence in point cloud modeling method's ability to estimate articular cartilage contact area

The purpose of this study is to demonstrate that an existing MRI modeling method can be successfully and accurately applied to estimate knee cartilage contact area in a single healthy adult and therefore can also be applied to subjects with knee OA. It is hypothesized that the MRI based method will produce estimates of cartilage contact area that are comparable to the literature.

1.4.2 Aim 2: Evaluate relationship between cartilage contact area and knee flexion in subjects with moderate knee OA and healthy, age matched controls

It is currently unknown how cartilage contact area changes with OA progression. Previous literature has shown that medial compartment cartilage contact area decreases with increasing knee flexion in healthy subjects (Tables 1.1,1.2). The MRI based method used in aim 1 will be applied to healthy and OA subjects across three flexion angles commonly encountered while weightbearing during gait. It is hypothesized that the healthy subjects will demonstrate the same relationship as the previous literature suggests, while the OA subjects will not due to changes resulting from cartilage degradation associated with the pathology.

1.5 References

1. Allaire R, Muriuki M, Gilbertson L, Harner CD. Biomechanical consequences of a tear of the posterior root of the medial meniscus. Similar to total meniscectomy. *J Bone Joint Surg Am*. 2008;90(9):1922-31.

2. Altman R, Asch E, Bloch D, Bole G, Borenstein D, Brandt K, Christy W, Cooke TD, Greenwald R, Hochberg M, Howell D, Kaplan D, Koopman W, Longley S, Mankin H, McShane DJ, Medsger T, Meenan R, Mikkelsen W, Moskowitz R, Murphy W, Rothschild B, Segal M, Sokoloff L, Wolfe F. Development of criteria for the classification and reporting of osteoarthritis. *Arthritis Rheum*. 1986;29(8):1039-49.

3. American Academy of Orthopaedic Surgeons. Osteoarthritis of the knee: evidence-based resources [Internet]. Rosemont (IL):American Academy of Orthopaedic Surgeons; 2004.

4. American Academy of Orthopaedic Surgeons. Osteoarthritis of the knee: state of the condition [Internet]. Rosemont (IL):American Academy of Orthopaedic Surgeons; 2004.

5. American Academy of Orthopaedic Surgeons. Osteoarthritis of the knee: treatment options [Internet]. Rosemont (IL):American Academy of Orthopaedic Surgeons; 2004.

6. Amin S, LaValley MP, Guermazi A, Grigoryan M, Hunter DJ, Clancy M, Niu JB, Gale DR, Felson DT. The relationship between cartilage loss on magnetic resonance imaging and radiographic progression in men and women with knee osteoarthritis. *Arthritis Rheum*. 2005;52(10):3152-9.

7. Andriacchi TP, Mundermann A, Smith RL, Alexander EJ, Dyrby CO, Koo S. A Framework for the in vivo pathomechanics of osteoarthritis at the knee. *Ann Biomed Eng*. 2004;32(3):447-57.

8. Arokoski JP, Jurvelin JS, Väätäinen U, Helminen HJ. Normal and pathological adaptations of articular cartilage to joint loading. *Scand J Med Sci Sports*. 2000;10(4):183-5.

9. Asano T, Akagi M, Tanaka K, Tamura J, Nakamura T. In vivo three-dimensional knee kinematics using a biplanar image-matching technique. *Clin Orthop Relat Res*. 2001;388:157-66.

10. Bei Y, Fregly B. Multibody dynamic simulation of knee contact mechanics. *Med Eng Phys*. 2004;26(9):777-89.

11. Berthiaume MJ, Raynauld JP, Martel-Pelletier J, Labonte F, Beaudoin G, Bloch DA, Choquette D, Haraoui B, Altman RD, Hochberg M, Meyer JM, Cline GA, Pelletier JP. Meniscal tear and extrusion are strongly associated with progression of symptomatic knee osteoarthritis as assessed by quantitative magnetic resonance imaging. *Ann Rheum Dis*. 2005;64(4):556-63.

12. Besier TF, Draper CE, Gold GE, Beaupré GS, Delp SL. Patellofemoral joint contact area increases with knee flexion and weight-bearing. *J Orthop Res.* 2005;23:345-50.

13. Bingham JT, Papannagari R, Van de Velde SK, Gross C, Gill TJ, Felson DT, Rubash HE, Li G. In vivo cartilage contact deformation in the healthy human tibiofemoral joint. *Rheumatology (Oxford).* 2008;47:1622-7.

14. Brandt KD, Dieppe P, Radin EL. Etiopathogenesis of osteoarthritis. *Rheum Dis Clin North Am*. 2008;34:531-59.

15. Buckwalter JA, Saltzman C, Brown T. The impact of osteoarthritis: Implications for Research. *Clin Orthop Relat Res*. 2004;427S: S6-15.

16. Cicuttini F, Hankin J, Jones G, Wluka A. Comparison of conventional standing knee radiographs and magnetic resonance imaging in assessing progression of tibiofemoral joint osteoarthritis. *Osteoarthritis Cartilage*. 2005;13(8):722-7.

17. Cooper C, Snow S, McAlindon TE, Kellingray S, Stuart B, Coggon D, Dieppe PA. Risk factors for the incidence and progression of radiographic knee osteoarthritis. *Arthritis Rheum*. 2000;43(5):995-1000.

18. DeFrate LE, Sun H, Gill TJ, Rubash HE, Li G. In vivo tibiofemoral contact analysis using 3d MRI-based knee models. *J Biomech*. 2004;37(10):1499-504.

19. Donahue TL, Hull ML, Rashid MM, Jacobs CR. A finite element model of the human knee joint for the study of tibio-femoral contact. *J Biomech Eng*. 2002;124(3):273-80.

20. Eckstein F, Glaser C. Measuring cartilage morphology with quantitative magnetic resonance imaging. *Semin Musculoskelet Radiol*. 2004;8(4):329-53.

21. Federico S, La Rosa G, Herzog W, Wu JZ. Effect of fluid boundary conditions on joint contact mechanics and applications to the modeling of osteoarthritic joints. *J Biomech Eng*. 2004;126:220-5.

22. Felson DT, Zhang YQ. An update on the epidemiology of knee and hip osteoarthritis with a view to prevention. *Arthritis Rheum*. 1998;41(8):1343-55.

23. Felson. DT. Developments in the clinical understanding of osteoarthritis. *Arthritis Res Ther*. 2009;11(1):203.

24. Fukubayashi T, Kurosawa H. The contact area and pressure distribution pattern of the knee: a study of normal and osteoarthrotic knee joints. *Acta Orthop Scand*. 1980;51(6):871-9.

25. Gandy SJ, Dieppe PA, Keen MC, Maciewicz RA, Watt I, Waterton JC. No loss of cartilage volume over three years in patients with knee osteoarthritis as assessed by magnetic resonance imaging. *Osteoarthritis Cartilage*. 2002;10(12):929-37.

26. Gold GE, Beaulieu CF. Future of MR imaging of articular cartilage. *Semin Musculoskelet Radiol*. 2001;5(4):313-27.

27. Gold GE, Besier TF, Draper CE, Asakawa DS, Delp SL, Beaupre GS. Weight-bearing MRI of patellofemoral joint cartilage contact area. *J Magn Reson Imaging*. 2004;20(3):526-30.

28. Hamilton N, Luttgens K. *Kinesiology: Scientific Basis of Human Motion.* 10th ed. New York (NY): McGraw-Hill; 2002. p. 183-93.

29. Hill PF, Vedi V, Williams A, Iwaki H, Pinskerova V, Freeman MA. Tibiofemoral movement 2: the loaded and unloaded living knee studied by MRI. *J Bone Joint Surg Br*. 2000;82(8):1196-8.

30. Hinterwimmer S, Gotthardt M, von Eisenhart-Rothe R, Sauerland S, Siebert M, Vogl T, Eckstein F, Graichen H. In vivo contact areas of the knee in patients with patellar subluxation. *J Biomech*. 2005;38(10):2095-101.

31. Hunter DJ, Niu JB, Felson DT, Harvey WF, Gross KD, McCree P, Aliabadi P, Sack B, Zhang YQ. Knee alignment does not predict incident osteoarthritis - the Framingham osteoarthritis study. *Arthritis Rheum*. 2007;56(4):1212-18.

32. Kellgren JH, Lawrence JS. Radiological assessment of osteo-arthritis. *Ann Rheum Dis*. 1957;16:494-502.

33. Kettelkamp DB, Jacobs AW. Tibiofemoral contact area – determination and implications. *J Bone Joint Surg A*. 1972;54(2):349-56.

34. Lee SJ, Aadalen KJ, Malaviya P, Lorenz EP, Hayden JK, Farr J, Kang RW, Cole BJ. Tibiofemoral contact mechanics after serial medial meniscectomies in the human cadaveric knee. *Am J Sports Med*. 2006;34(8):1334-44.

35. Li G, DeFrate LE, Park SE, Gill TJ, Rubash HE. In vivo articular cartilage contact kinematics of the knee: An investigation using dual-orthogonal fluoroscopy and magnetic resonance image-based computer model. *Am J Sports Med*. 2005;33(1):102-7.

36. Martel-Pelletier J, Boileau C, Pelletier JP, Roughley PJ. Cartilage in normal and osteoarthritis conditions. *Best Pract Res Clin Rheumatol*. 2008;22(2):351-84.

37. Miyazaki T, Wada M, Kawahara H, Sato M, Baba H, Shimada S. Dynamic load at baseline can predict radiographic disease progression in medial compartment knee osteoarthritis. *Ann Rheum Dis.* 2002;61(7):617-22.

38. Moro-oka TA, Hamai S, Miura H, Shimoto T, Higaki H, Fregly BJ, Iwamoto Y, Banks SA. Dynamic activity dependence of in vivo normal knee kinematics. *J Orthop Res*. 2008;26(4):428-34.

39. Niu J, Zhang YQ, Torner J, Nevitt M, Lewis CE, Aliabadi P, Sack B, Clancy M, Sharma L, Felson DT. Is obesity a risk factor for progressive radiographic knee osteoarthritis? *Arthritis Care Res*. 2009;61(3):329-35.

40. North Carolina School of Science and Mathematics [Internet]. Durham, NC. Experience NCSSM; [cited 2009 Nov 3]. Available from: http://www.ncssm.edu/library/dirt/Valerie%20Todd/Basic%20Anatomy.html

41. Patel VV, Hall K, Ries M, Lotz J, Ozhinsky E, Lindsey C, Lu Y, Majumdar S. A three-dimensional MRI analysis of knee kinematics. *J Orthop Res*. 2004;22(2):283-92.

42. Pelletier JP, Raynauld JP, Berthiaume MJ, Abram F, Choquette D, Haraoui B, Beary JF, Cline GA, Meyer JM, Martel-Pelletier J. Risk factors associated with the loss of cartilage volume on weight-bearing areas in knee osteoarthritis patients assessed by quantitative magnetic resonance imaging: a longitudinal study. *Arthritis Res Ther*. 2007;9(4):R74.

43. Périé D, Hobatho MC. In vivo determination of contact areas and pressure of the femorotibial joint using non-linear finite element analysis. *Clin Biomech*. 1998;13(6):394-402.

44. Potter HG, Foo LF. Magnetic resonance imaging of articular cartilage: trauma, degeneration, and repair. *Am J Sports Med.* 2006;34(4):661-77.

45. Raynauld JP, Kauffmann C, Beaudoin G, Berthiaume MJ, de Guise JA, Bloch DA, Camacho F, Godbout B, Altman RD, Hochberg M, Meyer JM, Cline G, Pelletier JP, Martel-Pelletier J. Reliability of a quantification imaging system using magnetic resonance images to measure cartilage thickness and volume in human normal and osteoarthritic knees. *Osteoarthritis Cartilage*. 2003;11(5):351-60.

46. Raynauld JP, Martel-Pelletier J, Berthiaume MJ, Beaudoin G, Choquette D, Haraoui B, Tannenbaum H, Meyer JM, Beary JF, Cline GA, Pelletier JP. Long term evaluation of disease progression through the quantitative magnetic resonance imaging of symptomatic knee osteoarthritis patients: correlation with clinical symptoms and radiographic changes. *Arthritis Res Ther.* 2006;8(1):R21.

47. Recht M, Bobic V, Burstein D, Disler D, Gold G, Gray M, Kramer J, Lang P, McCauley T, Winalski C. Magnetic resonance imaging of articular cartilage. *Clin Orthop Relat Res.* 2001;391:S379-96.

48. Shefelbine SJ, Ma CB, Lee KY, Schrumpf MA, Patel P, Safran MR, Slavinsky JP, Majumdar S. MRI analysis of in vivo meniscal and tibiofemoral kinematics in ACL-deficient and normal knees. *J Orthop Res*. 2006;24(6):1208-17.

49. Stammberger T, Eckstein F, Englmeier KH, Reiser M. Determination of 3d cartilage thickness data from MR imaging: computational method and reproducibility in the living. *Magn Reson Med*. 1999;41(3):529-36.

50. Wluka AE, Stuckey S, Snaddon J, Cicuttini FM. The Determinants of change in tibial cartilage volume in osteoarthritic knees. *Arthritis Rheum*. 2002;46(8):2065-72.

51. Wretenberg P, Ramsey DK, Németh G. Tibiofemoral contact points relative to flexion angle measured with MRI. *Clin Biomech*. 2002;17(6):477-85.

52. Wu JZ, Herzog W, Epstein M. Joint contact mechanics in the early stages of osteoarthritis. *Med Eng Phys*. 2000;22(1):1-12.

53. Zhao D, Banks SA, Mitchell KH, D'Lima DD, Colwell CW Jr, Fregly BJ. Correlation between the knee adduction torque and medial contact force for a variety of gait patterns. *J Orthop Res*. 2007;25(6):789-97

Chapter 2

METHODS

2.1 Introduction

A series of three assessments were performed in order to establish confidence in the knee modeling method's ability to estimate contact area. The method's ability to generate repeatable data, sensitivity to cartilage tracings, and intra-observer reliability were assessed. Articular cartilage contact area and its relationship with knee flexion was also investigated in a cohort of moderate OA subjects and healthy controls.

2.2 Subjects

Data were collected on 31 subjects recruited from the local community through advertisements and word of mouth. In order to participate in our study, subjects were required to have radiographic evidence of moderate knee OA (KL = 2-3), the ability to walk for five minutes at self selected speed, be 30-85 years of age, and have a body mass index (BMI) less than 35. Exclusion criteria included: congestive heart failure, peripheral artery disease with claudication, cancer, pulmonary or renal failure, unstable angina, uncontrolled hypertension, neurological disorder, current pregnancy, OA due to significant bony deformity, ACL-deficiency, laterally dominant (LC KL grade > MC KL grade) knee OA, and diagnosed arthritis of other lower extremity joints. Subjects were also required to have no contraindications for MRI

collection which include: claustrophobia, presence of aneurysm clips, ear or eye implants, work in or around sheet metal, have metal hair accessories, and have any sort of magnetic metal in their body (i.e. shrapnel). The healthy age-matched controls were also subject to the same inclusion and exclusion criteria, but were required to have no radiographic evidence of knee OA (KL = 0-1).

2.3 Data collection process

The protocol was approved by the Human Subject Review Board at the University of Delaware and prior to participating in the study, all subjects completed an informed consent form and health questionnaire. Semi-flexed anteroposterior radiographs of both knees were collected at a local imaging clinic (Papastavros' Associates Medical Imaging, Newark, DE). The radiographs were assessed by an experienced radiologist for KL grade on the medial and lateral compartments of both knees. A separate data collection session was performed at a local MRI clinic (Diagnostic Imaging Associates: Brandywine, Wilmington, DE). Data were collected in an open MRI scanner (Stand-Up™, Fonar Corporation, Melville, NY) which allowed for approximately full weightbearing. Scans of each knee were conducted with the scanning table almost vertical (85°) with the knee in full extension. Three scans of each knee were also collected during partial weightbearing (table at 45°) with the knee in full extension and 15° and 30° relative knee flexion.

Knee flexion was assessed and maintained during scanning through the use of a custom knee positioning device (Figure 2.1). Prior to entering the imaging room, knee flexion angles and resultant knee positioning measurements were taken. The back of the knee positioning device was placed next to a wall and the subject was instructed to stand on the device with the cantilever beam portion between their legs

and their heels pressed gently against the base of the device. The subjects were then instructed to stand "as straight as possible" and point their feet forward for the assessment of full extension of the knee. Once the subject complied, the bony landmarks of the greater trochanter of the femur, lateral malleolus of the ankle, and an estimate of the knee joint center were used to approximate the knee flexion angle with a handheld goniometer. Once the flexion angle was recorded, the measuring arm was placed on the device and it was aligned to gently press against the patella of the knee and the corresponding distance was recorded. Increments of 15° were added to the goniometer reading as the subject's knee was repositioned in order to achieve 15° and 30° relative knee flexion and the distance was recorded. The process was completed for both legs. Once this was completed, the cantilever beam portion of the knee positioning device was affixed to the table in the MRI scanner to recreate the hallway positioning. The heelboard was necessary due to a gap of approximately ½" between the back of the scanning table and the base of the table where the subject stood in order to best maintain a physiologically meaningful standing position. During each scan the measuring arm was set to the corresponding distance and the subject's knee flexion was adjusted. The subject was instructed to maintain contact with the device in order to maintain the appropriate knee flexion angle and help limit drift during the scan, however they were also instructed not to apply pressure to the device.

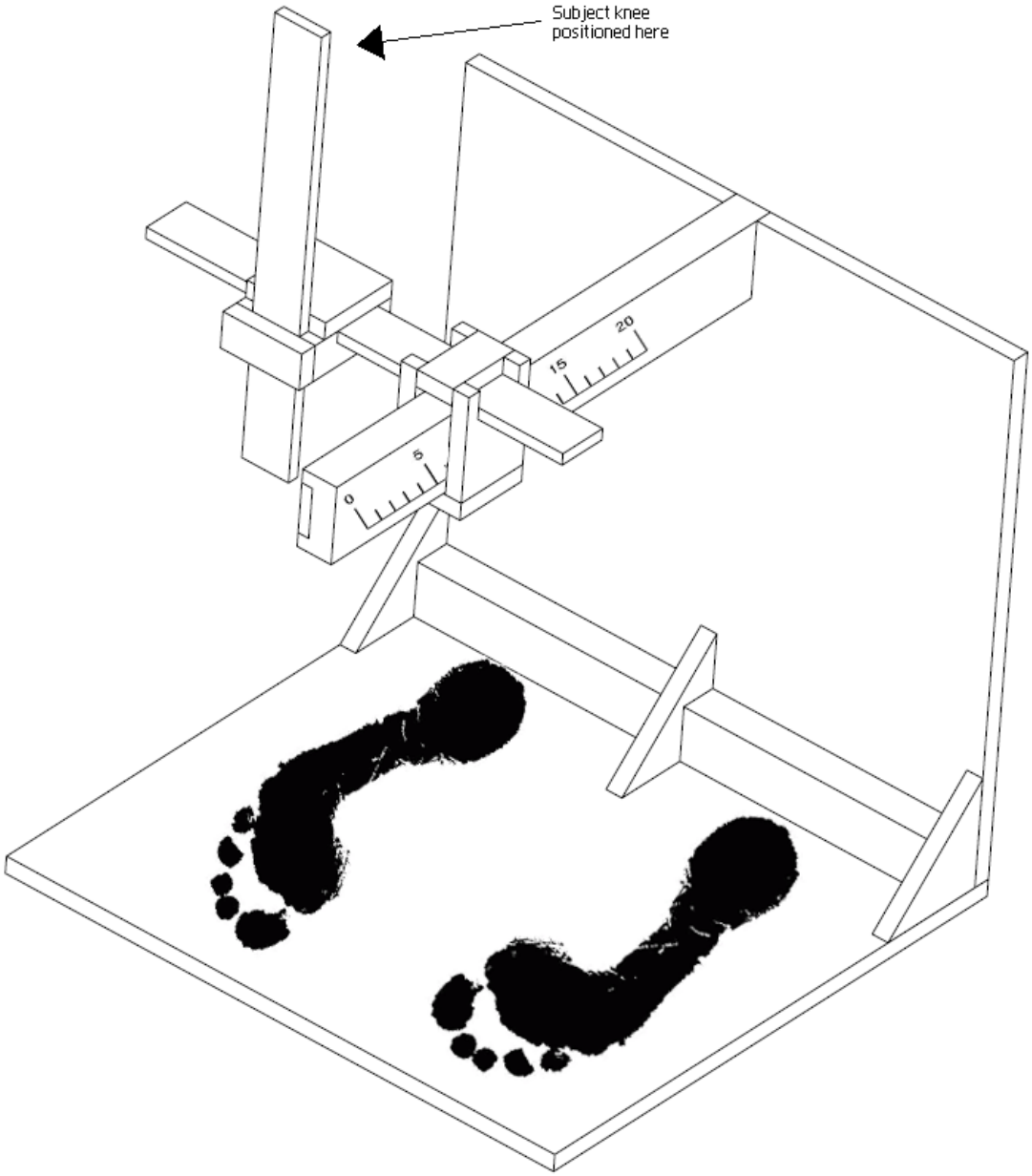

Figure 2.1 Schematic of custom knee positioning device showing subject positioning

In preparation for the scan, subjects were instructed to distribute their weight equally between their legs and stand still for the entire duration of the scan. A preliminary scouting scan was first conducted in which single sagittal, coronal, and transverse plane images were taken. This scout scan was used to orient the MRI slices along the long axis of the femur. The sagittal plane MRIs collected used a T1 fast spin echo sequence and consisted of 30 slices with a slice thickness of 3.0 mm, a 3.3 mm interval between slices, a field of view of 25 cm, echo time of 20 ms, a repetition time of 355 ms, and a display matrix of 512 x 512. The full weightbearing scan of a randomly selected leg was first collected, followed by the three partial weightbearing scans in a random order. After all four scans had been collected on a single leg, subjects were allowed a rest break if they desired before data were similarly collected on the other leg. Calibration and data collection for each of the eight MRI sequences lasted approximately 6.5 minutes and an entire data collection lasted approximately 2 hours.

2.4 Excluded data

The data from nine subjects were excluded from analysis. Three subjects had severe OA (KL = 4), three subjects were found to have laterally dominant OA, two subjects did not meet the age criteria, and one subject generated extremely poor resolution MRIs. A total of 11 moderate OA subjects and 11 healthy controls were included in the data analysis.

2.5 Image preparation

The acquired MRI data have embedded scan and subject parameters. During the process of importing the data to the processing computer, all personal and

identifying information were removed and replaced with a subject number in order to maintain subject anonymity. The MRI data were compiled into an appropriate format using custom written MATLAB (MathWorks, Natick, MA) code in order to import the data into the IMOD software (University of Colorado, CO) for digitizing.

2.6 Digitization process and coordinate system assignment

The distal femur, proximal tibia, proximal fibula, and medial and lateral cartilage of the femur and tibia were traced on a digitizing tablet (Wacom Technology Corporation, Vancouver, WA) in IMOD by a single observer. Medial and lateral sections of the tibiofemoral joint were separated by the femoral notch. In order for a surface to be traced on a given image, clear distinction of its edge had to be apparent; the use of adjacent images to assist in identifying the edges of the surfaces of interest was allowed. Bony landmarks were also identified on a single scan (right leg, full weightbearing) in order to apply an established joint coordinate system (5). The medial-lateral axis of the femur was established by locating the center of the lateral epicondyle on the most lateral sagittal image that it appeared with the center of the medial femoral epicondyle on the most medial slice that it appeared. The longitudinal axis of the femur was determined by selecting a mid-sequence slice that had minimal thinning of the femur towards the proximal end and digitizing a pair of points on both the proximal and distal ends of the femoral shaft. Within each pair of points, one point identified the anterior side of the femur and the other established the posterior boundary. The vector created by connecting the midpoint of each pair was used to establish the longitudinal axis. The third axis was obtained by taking the cross product of the first two. The femoral notch was also digitized and served as the origin for the femoral coordinate system. The tibial coordinate system was established in a similar

manner. The medial-lateral axis was generated by connecting the midpoint of the most medial slice that showed the tibial plateau with the midpoint of the most lateral slice that still visualized the tibial plateau. The long axis of the tibia was determined by a vector connecting a single point on the proximal posterior aspect of the tibia with another on the posterior distal portion of the tibia. The third axis was generated as the cross-product between the medial-lateral and long axis of the tibia. The tibial coordinate system originated on the peak of the medial tibial spine. The accuracy of the coordinate systems was visually confirmed using a MATLAB routine that allowed for viewing of the three dimensional bone model with coordinate systems attached. A tibial plateau coordinate system was also generated using the medial-lateral tibial coordinate system and an anterior-posterior axis generated from digitized reference points along the lateral aspect of the tibial plateau.

2.7 Generation of reference knee joint model and application to other scans

The MRI tracings were imported into a custom MATLAB code to generate a point cloud data set of each of the bones. These point clouds were then compared with the data generated from a reference MRI (right knee at full extension and weightbearing) using the trimmed iterative closest point algorithm (TrICP) (3). The TrICP is able to create a model that is superior to the traditional iterative closest point algorithm by discarding digitized points that are too far removed from the reference model data to be considered plausible prior to using the point cloud data set to generate bony geometry of the knee (1). Fitting each bone model within a given subject to its corresponding reference bone model allows for appropriate application of the femoral and tibial coordinate systems to all scans of that subject.

2.8 Contact area determination

Contact area for the medial and lateral compartments of the tibiofemoral joint was considered separately. In each compartment, the digitized cartilage of the tibia was used to generate a two dimensional mesh of 100 by 100 points along a surface generated by the tibial plateau coordinate system (z = 0). The area within each grid space was extruded vertically to the surface of the tibial cartilage. Custom MATLAB routines implemented a kd-tree sorting algorithm to search for femoral cartilage points nearest to the tibial cartilage surface that encompasses that grid space. The kd-tree algorithm decreases computing time by only checking the distance to nearby femoral cartilage points rather than each data point in the femoral cartilage surface. A previous study established an "in-plane resolution" for MRI based studies that quantifies their accuracy based on scan parameters (4). The scan parameters of our study dictated a threshold distance of 0.5 mm be used for determining articular cartilage contact area. If any point on the tibial cartilage surface within the grid space was within 0.5 mm of femoral cartilage, the entire grid space was deemed to be in contact. Cartilage surfaces were retraced after a period of two weeks had passed and articular cartilage contact area estimates are reported as an average of these two tracings.

2.9 Normalization of the data

Articular cartilage contact area estimates were normalized to an approximation of the tibial plateau in order to account for discrepancies in joint size between subjects. The data points that comprised the tibial plateau were input into a custom written MATLAB routine that approximated the length of the tibial plateau along the anterior-posterior and medial-lateral axes. For each axis, all of the points

that fell within 0.5 mm of either side of the axis were identified and the most distal point in both the positive and negative direction was identified. The average of each pair of points was taken and the distance between the two sets of points along a single axis was used to estimate its length. The tibial plateau was estimated to be approximately rectangular and as a result, a normalized value for the articular cartilage contact area was estimated by dividing the raw contact area by the product of the lengths of the two axes (Figure 2.2) similar to a previous study that investigated patellofemoral cartilage contact area (2).

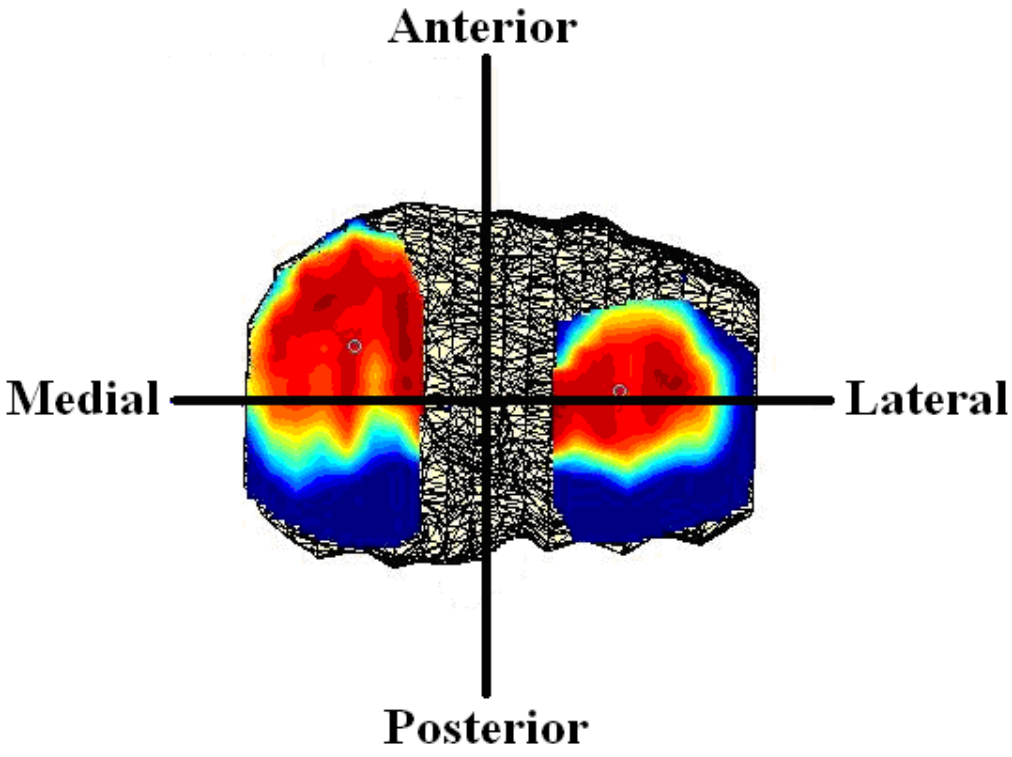

Figure 2.2 Superior surface of tibial plateau with anterior-posterior and medial-lateral axes drawn. The product of the length of each axis along the surface of the tibial plateau was used to normalize the articular cartilage contact area data.

2.10 Conclusions

MRI data were collected on 31 subjects. Data from a single healthy subject were used to assess the knee modeling method's ability to estimate articular cartilage contact area. The relationship between articular cartilage contact area and knee flexion was analyzed in moderate OA subjects (n = 11) and healthy controls (n = 11).

2.11 References

1. Barrance PJ, Pepe TM, Buchanan TS. In Vivo Knee Kinematics Measured in Weight-Bearing Flexion Using Standing Magnetic Resonance Imaging. *Proceedings of the 2005 Summer Bioengineering Conference*; 2005 Jun 22-26: Vail (CO). 2005.

2. Besier TF, Draper CE, Gold GE, Beaupré GS, Delp SL. Patellofemoral joint contact area increases with knee flexion and weight-bearing. *J Orthop Res*. 2005;23(2): 345-50.

3. Chetverikov D, Stepanov D, Krsek P. Robust euclidean alignment of 3D point sets: the trimmed iterative closest point algorithm. *Image Vis Comput*. 2005;23(3):299-309.

4. Cohen ZA, McCarthy DM, Kwak SD, Legrand P, Fogarasi F, Ciaccio EJ, Ateshian GA. Knee cartilage topography, thickness, and contact areas from MRI: in-vitro calibration and in-vivo measurements. *Osteoarthritis Cartilage.* 1999;7(1):95-109.

5. Grood ES, Suntay WJ. A Joint Coordinate System for the Clinical Description of Three-Dimensional Motions: Application to the Knee. *J Biomech Eng.* 1983;105(2):136-44.

Chapter 3

AIM 1: IMPLEMENT AND ESTABLISH CONFIDENCE IN POINT CLOUD MODELING METHOD'S ABILITY TO ESTIMATE ARTICULAR CARTILAGE CONTACT AREA

3.1 Introduction and background

Knee OA is a pathological condition that is characterized by a narrowing of the joint space between the tibia and femur. It has been shown to affect approximately 12 % of people greater than 60 years of age (6) and estimates of annual medical and lost work expenses due to osteoarthritis are greater than $60 billion in the United States alone (4).

Previous investigators have suggested that OA represents a failure of the joint to perform necessary cellular maintenance due to excessive mechanical stress (3). In a simplified case, mechanical stress is directly proportional to the load applied across the joint and inversely proportional to contact area. Consequently, increased stress can be due to increased load or decreased contract area. Data from an instrumented prosthesis have shown that a significant correlation exists between medial contact force and knee adduction moment (15), while another study has identified an increased knee adduction moment as a risk factor for progression of knee OA (12). The results from these studies support the idea that axial loading is a key component in OA progression; however the relationship between contact area and OA progression is not well understood. Contact area may change in OA due to any

combination of factors including: increased cartilage compliance, meniscal extrusion, cartilage degradation, or osteophyte formation.

Cadaveric studies involving the use of pressure sensitive film have been a popular *in vitro* modality for studying tibiofemoral contact area in the past (7,11). Implications from these studies were limited by the removal of surrounding soft tissues and application of physiologically irrelevant loads. More recently MRI has been used as a tool to assess knee joint contact area *in vivo*. Studies of knee joint contact area have been performed in several pathological populations including patellar subluxations (10) and anterior cruciate ligament (ACL) deficiencies (14); however to the best of the investigators knowledge, no *in vivo* studies have measured articular cartilage contact area in the knee OA population.

Previous MRI based studies have estimated cartilage contact area by manually identifying areas of the articular cartilage that appear to be in contact and multiplying this measure by the slice thickness (2,8,13,14). This methodology is not ideal as the accuracy of the contact area measure is dependent on the through plane resolution (slice spacing).

In this study, we will apply a MRI based tibiofemoral modeling method to estimate articular cartilage contact area. This method improves on previous methods in that it generates a three dimensional model that is used to estimate cartilage contact area rather than summing the contact area over a set of two dimensional images. This method has been previously validated for the measurement of joint kinematics (1). It is hypothesized that the method will produce measurements of articular cartilage contact area in a single healthy subject similar to those found in the literature.

3.2 Methods

A single healthy female subject was recruited from the local community for participation in this study. The characteristics of this subject can be seen in Table 3.1. Approval of this study was granted by the University of Delaware's Human Subjects Review Board and the subject signed an informed consent form prior to participating.

Table 3.1 Subject characteristics

Age (yrs)	52
Height (m)	1.68
Weight (kg)	72.3
BMI (kg/m^2)	25.7

Imaging data were acquired using a 0.6 T open MRI scanner (Stand-Up™, Fonar Corporation, Melville, NY). T1 fast spin echo sequence, weightbearing scans comprised of thirty 3 mm thick sagittal slices, spaced 3.3 mm apart, with a field of view of 25 cm, echo time of 20 ms, repetition time of 355 ms and a display matrix of 512 x 512 were acquired in approximately six and a half minutes. Scans of both knees were acquired in full knee extension at approximately full weightbearing (table at 85°) and partial weightbearing (table at 45°). Partial weightbearing scans were also acquired with 15° and 30° relative knee flexion. Data collection for the eight MRIs lasted approximately two hours.

The MRIs were traced using a digitizing tablet (Wacom Technology Corporation, Vancouver, WA) and IMOD software (University of Colorado, CO). Distal femoral, proximal tibial¸ and their respective medial and lateral compartment articular cartilage surfaces were identified. The medial and lateral compartments were

separated by the sagittal MRI slice that contained the femoral notch. The digitized points were input into a three dimensional modeling method that has been previously validated for its kinematic measures (1). The modeling method used the trimmed iterative closest point algorithm (5) which is an improvement over the traditional iterative closest point algorithm in that it is able to discard points that are deemed unrealistic for the expected bony geometries from a subject specific reference MRI. Joint coordinate systems were applied to determine actual knee flexion angles (9).

Articular cartilage contact area was estimated for each compartment independently. A two dimensional 100 by 100 grid was created from the tibial cartilage of the respective compartment. Within each grid space, the minimum distance from the surface of the tibial cartilage to the surface of the nearest femoral cartilage was determined. If the minimum distance was not greater than 0.5 mm, the grid space was estimated to be in contact.

3.2.1 Solution uniqueness

Since the algorithm implemented by the modeling method discarded points, it was necessary to determine whether it consistently removed the same points. This was assessed by modeling the same set of digitized points four times.

3.2.2 Method sensitivity

Subject motion during imaging has the potential to generate sub-optimal images, which in turn can make it difficult to accurately assess the cartilage surfaces. The method's sensitivity to this motion was evaluated by removing tibial and femoral cartilage digitizations on image slices and evaluating their effect on the articular cartilage contact area estimate. The images that comprised the medial compartment

were separated into thirds (medial, middle, lateral) and within each third four variations of cartilage tracings were deleted: tibial cartilage on one slice, femoral cartilage on one slice, both tibial and femoral cartilage on one slice, and both tibial and femoral cartilage on two slices.

3.2.3 Intra-observer reliability

Reliability of the manual tracings was assessed by retracing the set of MRIs after a period of 30 days had passed. The articular cartilage contact area estimates were compared and the correlation coefficient was used to estimate intra-observer reliability. Mean CVs for each compartment were also determined.

3.3 Results

3.3.1 Solution uniqueness

Across all four models, it was found that identical estimates of articular cartilage contact area were calculated.

3.3.2 Method sensitivity

The results from the assessment of sensitivity of the method are shown in Table 3.2 as a percentage difference from the original baseline contact area estimate. Decreases in medial compartment articular cartilage contact area estimates of 3.2 to 28.6 % across both knees were seen in the medial third, while the contact area estimate increased slightly in some permutations and decreased 8.9 % maximally in the middle third. The lateral third of the medial compartment was found to be most sensitive to the cartilage tracings. Deletions of cartilage surfaces in this third were found to decrease the compartment cartilage contact area 19.2 to 49.3 %.

Table 3.2 Results of evaluation of method sensitivity. Modeling method was found to be most sensitive to cartilage tracings on the periphery of the compartment.

	Slices with tibial cartilage removed	Slices with femoral cartilage removed	Percent difference from baseline		
			Right knee	Left knee	Average
Medial 1/3	1	0	10.7	3.9	10.6
	0	1	9.0	3.2	
	1	1	10.7	3.8	
	2	2	28.6	15.3	
Middle 1/3	1	0	-1.7	5.7	2.4
	0	1	3.8	-2.4	
	1	1	1.6	0.7	
	2	2	2.8	8.9	
Lateral 1/3	1	0	25.0	20.1	27.6
	0	1	22.2	19.2	
	1	1	24.9	20.7	
	2	2	49.3	39.2	

3.3.3 Intra-observer reliability

The original tracings and re-tracings after 30 days had passed were found to have a correlation coefficient of 0.86 for the eight scans of the medial compartment and 0.95 when the contact area estimates of both compartments were considered (Figure 3.1). Mean coefficient of variations (CV) of the medial and lateral compartments were found to be 15.1 % and 19.9 %, respectively. At full weightbearing and full extension, mean articular cartilage contact areas of 511.0 ± 143.1 mm^2 and 256.4 ± 40.3 mm^2 were found for the medial and lateral compartments of both knees, respectively. Partial weightbearing scans (shown in Figure 3.2) demonstrated a decrease in both medial and lateral compartment articular cartilage contact area with increasing knee flexion.

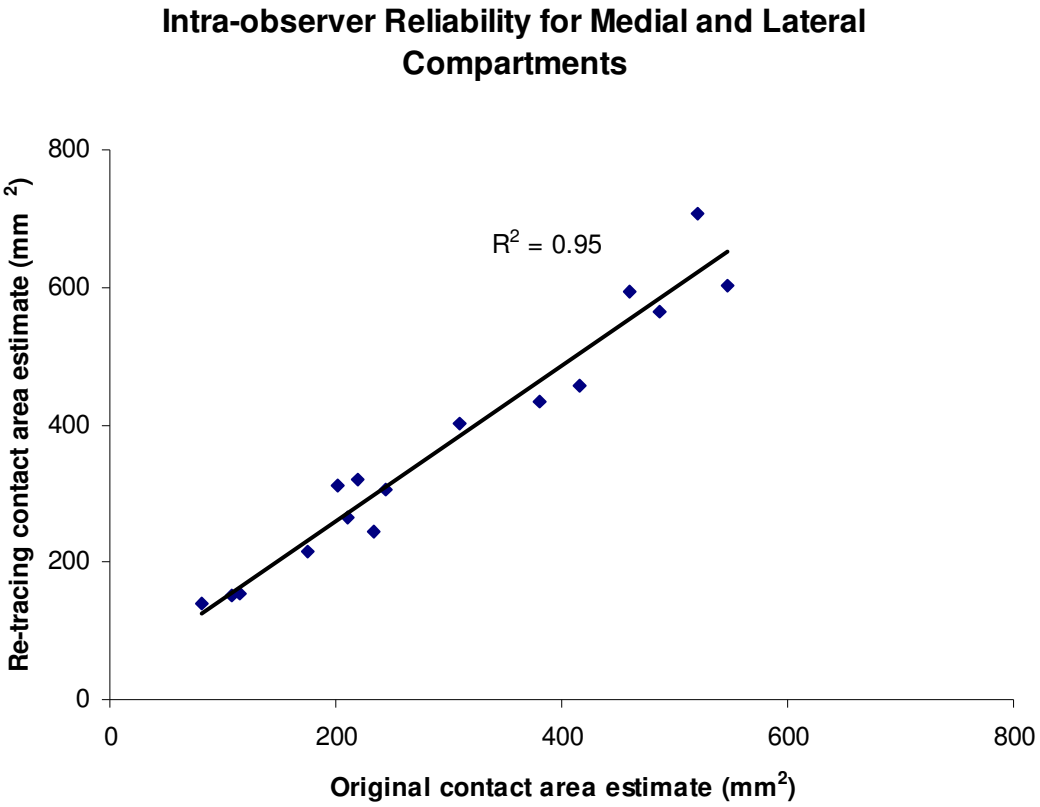

Figure 3.1 Correlation of two tracings of same MRI set after 30 days had passed

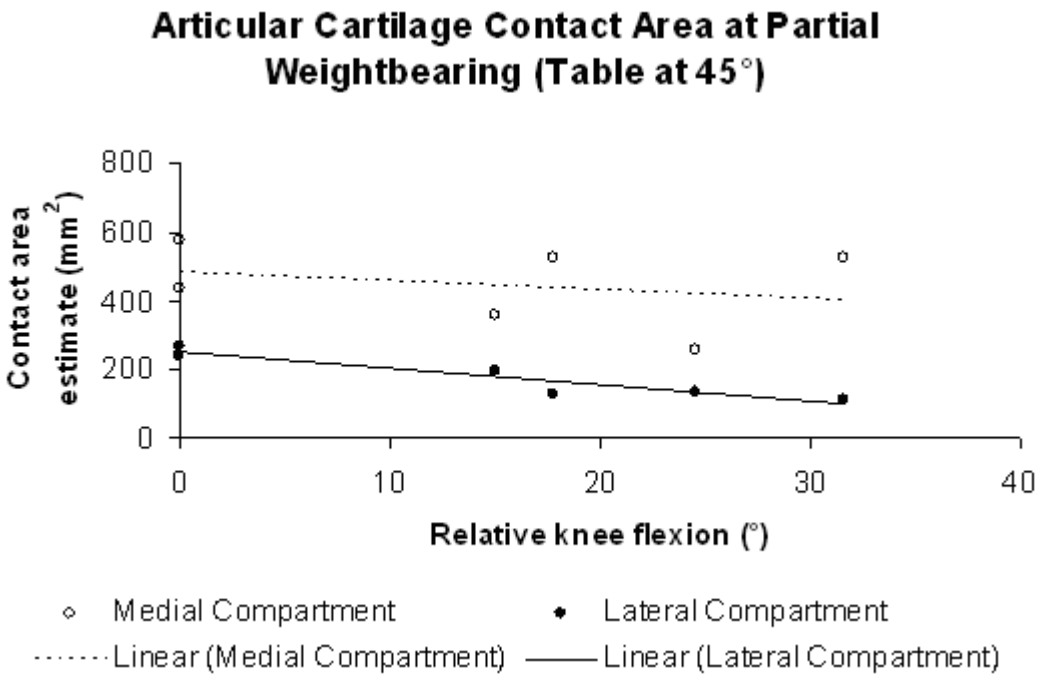

Figure 3.2 Articular cartilage contact area estimate at partial weightbearing. Points represent mean of original and retracing. Both compartments demonstrate a decrease in articular cartilage contact area with increasing knee flexion.

3.4 Discussion

3.4.1 Solution uniqueness

The modeling method was found to generate a unique solution when the same set of tracings was input. This is advantageous because it demonstrates that the trimmed iterative closest point algorithm does not involve any form of optimization where there is concern of generating a family of solutions.

3.4.2 Method sensitivity

Cartilage tracings on slices were deleted in order to simulate subject motion and evaluate the effect that this might have if the observer were unable to identify the surface on a particular slice. The results suggest that the outer sagittal slices of the compartment are most sensitive to incomplete cartilage tracings while deletions of cartilage in the middle third of the compartment have a relatively low effect on the method's ability to estimate articular cartilage contact. It is important to keep in mind that although this test did attempt to quantify the sensitivity of the method, it is highly unlikely that there would be enough motion for no cartilage surface to be traced on even a single slice. Subject motion could lead to incomplete cartilage digitization on a single slice, but would rarely if ever obscure the complete cartilage surface on a single slice. In the case of this single subject, all cartilage surfaces were completely traced.

3.4.3 Intra-observer reliability

Acceptable intra-observer reliability for cartilage contact area was found. Previous studies have reported mean CVs of 3.0 % for intra-observer reliability for the patellofemoral joint (8) and 5.0 % on a MRI phantom (13). Our overall mean CV of 17.5 % is much higher than previous studies; however the contact area we attempted to model had a much more complex geometry than previous investigators had used.

Our articular cartilage contact area estimate matches well with previous literature. In a MRI based study, Patel et al. (13) found contact areas of 374 mm^2 and 276 mm^2 for the medial and lateral compartments, respectively when a load of 133 N was applied axially to the bottom of the foot in 10 healthy subjects. Hinterwimmer et al. (10) estimated contact of 487 mm^2 in the medial compartment and 220 mm^2 in the

lateral compartment from non-weightbearing MRIs of 12 healthy subjects. Our contact area estimate is slightly higher than these studies, but this may be due to our subject's knee bearing a greater load (~365 N) than previous investigations. Decreasing articular cartilage contact area with increasing knee flexion in the medial compartment of the tibiofemoral joint has been seen previously in a cadaveric study (11) and MRI based investigations (10,13), while results on the effect of knee flexion on the articular cartilage contact area in the lateral compartment has been mixed. Previous investigations found that increasing knee flexion decreased (11), increased (10) or had a negligible effect (13) on lateral compartment contact area. It is also important to keep in mind that our results are from a single subject and incorporation of more subjects would increase confidence in our estimate of articular cartilage contact area and its relationship with knee flexion.

3.5 Conclusions

Tests to establish confidence in the ability of an existing MRI based knee modeling method to estimate articular cartilage contact area were performed. The method was found to yield a unique solution, be sensitive to incomplete cartilage digitizations on the peripheries of the compartment, and be repeatable. As a result of the high level of sensitivity to the cartilage digitizations, cartilage surfaces should be digitized and modeled twice, with an average taken to more closely estimate articular cartilage contact area. Data from a single, healthy subject were found to be comparable to previous studies. Future studies will apply this method to osteoarthritic joints in order to elucidate differences with the healthy population and garner an improved understanding of the differences in cartilage contact area that result from the pathology.

3.6 References

1. Barrance P, Pohl M, Noehren B, Barrios J, Davis I. Bone Surface Tracking for Standing Knee MRI: A Validation Study. *Proceedings of the 2007 American Society of Biomechanics Annual Conference*; 2007 Aug 22-25: Stanford (CA). Stanford University; 2007. p1-10.

2. Besier TF, Draper CE, Gold GE, Beaupré GS, Delp SL. Patellofemoral joint contact area increases with knee flexion and weight-bearing. *J Orthop Res*. 2005;23(2): 345-50.

3. Brandt KD, Dieppe P, Radin EL. Etiopathogenesis of Osteoarthritis. *Rheum Dis Clin North Am*. 2008;34(3):531-59.

4. Buckwalter JA, Saltzman C, Brown T. The Impact of Osteoarthritis: Implications for Research. *Clin Orthop Relat Res*. 2004;427S:S6-15.

5. Chetverikov D, Stepanov D, Krsek P. Robust euclidean alignment of 3D point sets: the trimmed iterative closest point algorithm. *Image Vis Comput*. 2005;23(3):299-309.

6. Felson DT, Zhang Y. An Update on the Epidemiology of Knee and Hip Osteoarthritis with a View to Prevention. *Arthritis Rheum*. 1998;41(8):1343-55.

7. Fukubayashi T, Kurosawa H. The Contact Area and Pressure Distribution Pattern of the Knee: A Study of Normal and Osteoarthrotic Knee Joints. *Acta Orthop Scand*. 1980;51(6):871-9.

8. Gold GE, Besier TF, Draper CE, Asakawa DS, Delp SL, Beaupre GS. Weight-Bearing MRI of Patellofemoral Joint Cartilage Contact Area. *J Magn Reson Imaging*. 2004;20(3):526-30.

9. Grood ES, Suntay WJ. A Joint Coordinate System for the Clinical Description of Three-Dimensional Motions: Application to the Knee. *J Biomech Eng*. 1983;105(2):136-44.

10. Hinterwimmer S, Gotthardt M, von Eisenhart-Rothe R, Sauerland S, Siebert M, Vogl T, Eckstein F, Graichen H. In vivo contact areas of the knee in patients with patellar subluxation. *J Biomech*. 2005;38(10):2095-101.

11. Kettelkamp DB, Jacobs AW. Tibiofemoral Contact Area – Determination and Implications. *J Bone Joint Surg A*. 1972;54(2):349-56.

12. Miyazaki T, Wada M, Kawahara H, Sato M, Baba H, Shimada S. Dynamic load at baseline can predict radiographic disease progression in medial compartment knee osteoarthritis. *Ann Rheum Dis*. 2002;61(7):617-22.

13. Patel VV, Hall K, Ries M, Lotz J, Ozhinsky E, Lindsey C, Lu Y, Majumdar S. A three-dimensional MRI analysis of knee kinematics. *J Orthop Res*. 2004;22(2):283-92.

14. Shefelbine SJ, Ma CB, Lee KY, Schrumpf MA, Patel P, Safran MR, Slavinsky JP, Majumdar S. MRI Analysis of In Vivo Meniscal and Tibiofemoral Kinematics in ACL-Deficient and Normal Knees. *J Orthop Res*. 2006;24(6):1208-17.

15. Zhao D, Banks SA, Mitchell KH, D'Lima DD, Colwell CW Jr, Fregly BJ. Correlation between the Knee Adduction Torque and Medial Contact Force for a Variety of Gait Patterns. *J Orthop Res*. 2007;25(6):789-97.

Chapter 4

AIM 2: EVALUATE RELATIONSHIP BETWEEN CARTILAGE CONTACT AREA AND KNEE FLEXION IN SUBJECTS WITH MODERATE KNEE OA AND HEALTHY, AGE MATCHED CONTROLS

4.1 Introduction and background

OA is a pathological condition characterized by joint degradation and causes disability in approximately 10% of people greater than 60 years. In the United States alone, OA costs $60 billion in medical expenses and lost wages annually (3).

Although the pathology is not well understood, it has previously been hypothesized that OA is related to a failure of the joint to maintain cellular homeostasis due to the applied mechanical stress (2). In a simplified case, mechanical stress is directly proportional to the axial load and inversely proportional to the cross-sectional area on which the load is distributed. In the tibiofemoral joint, the axial load can be approximated as the joint contact force, while the cross-sectional area can be approximated as the cartilage contact area. Through use of an instrumented prosthesis Zhao et al. (15) found that the medial compartment contact force correlated with the knee adduction moment during gait. The knee adduction moment has been previously found to significantly correlate with progression of knee OA (9) suggesting that the increased axial load in the medial compartment puts the subject at risk for progression.

Although previous literature supports the relationship between loading and OA progression, cartilage contact area in subjects with knee OA has not been extensively investigated, but will also influence mechanical stress. A single previous

study was found to investigate contact area in subjects with knee OA (5), however; the study included only two cadavers with non-quantified OA severity. Knee joint contact area has been studied *in vivo* previously in non-OA populations. Shefelbine et al. (13) used MRI to evaluate contact area in anterior cruciate ligament deficient subjects, Hinterwimmer et al. (7) studied subjects with patellar subluxation, and Patel et al. (10) studied young healthy adults. Decreases in medial compartment knee joint contact area of 9 and 17% were seen as knee flexion increased from 0° to 30° in Patel et al. (10) and Hinterwimmer et al. (7) studies, respectively.

Despite previous literature suggesting that cartilage volume decreases with increasing OA severity (12,14), no previous *in vivo* study has investigated whether cartilage contact area changes in the knee OA population. The hypothesized importance of mechanical stress in the joint leads us to believe that contact mechanics during the weightbearing phases of gait will provide important insights to the differences in joint stress between knee OA subjects and healthy controls. The purpose of this study was to use a MRI based modeling method to generate knee joint contact area estimates in subjects with knee OA and healthy controls and investigate changes in contact area across knee flexion angles used in the weightbearing phases of gait. It is hypothesized that the healthy subjects will demonstrate the same relationship as the previous literature suggests, while the OA subjects will not due to the cartilage breakdown associated with the pathology.

4.2 Methods

4.2.1 Subjects

Data were collected on 22 subjects recruited from the local community through advertisements and referrals. Inclusion criteria for the OA subjects consisted of radiographic evidence of moderate knee OA (KL grade = 2-3), the ability to walk for five minutes at self selected speed, 40-85 years of age, and have a BMI less than 35. Exclusion criteria included: congestive heart failure, peripheral artery disease with claudication, cancer, pulmonary or renal failure, unstable angina, uncontrolled hypertension, neurological disorder, current pregnancy, OA due to significant bony deformity, ACL-deficiency, laterally dominant knee OA, diagnosed arthritis of other lower extremity joints, or any contraindications for MRI. Healthy controls met similar criteria, but were required to have KL = 0-1. Approval for this study was granted by the University of Delaware's Institutional Review Board and all subjects completed an informed consent form prior to participation in the study.

4.2.2 Data acquisition

Semi-flexed anterior-posterior radiographs of both knees were collected at a local clinic (Papastavros' Associates Medical Imaging, Newark, DE) and read by an experienced radiologist. Medial and lateral compartments were scored separately resulting in four independent KL grades. During a separate data collection (Diagnostic Imaging Associates, Wilmington, DE), T1 fast spin-echo sequence MRIs of both knees were collected in a 0.6T open MRI scanner (Stand-Up™, Fonar Corporation, Melville, NY). The scans were comprised of thirty 3 mm thick sagittal images, spaced 3.3 mm apart, with a field of view of 25 cm, echo time of 20 ms, repetition time of 355 ms and a display matrix of 512 x 512. Calibration and data collection for each MRI lasted

approximately six and a half minutes. Scans were collected of each knee at full extension and a relative 15° and 30° knee flexion under partial weightbearing (table at 45°). The order of the scans was randomized for each subject and subjects were instructed to equally distribute their weight across both legs during the data acquisition process.

4.2.3 Data processing

The MRIs were manually traced on a digitizing tablet (Wacom Technology Corporation, Vancouver, WA) using IMOD software (University of Colorado, CO) by a single observer. The distal femur, proximal tibia, and their respective medial and lateral compartment articular cartilage surfaces were identified. Medial and lateral compartments were separated by the sagittal image that best showed the femoral notch. The digitized tracings were imported into a previously described knee modeling method (1). In short, the modeling method uses the TrICP (4) to match the digitized tracings of the femur and tibia to a subject specific model of the bones generated from a reference MRI. Points deemed unrealistic for the expected geometry were discarded, while the cartilage tracings were left unaltered. Bony landmarks were identified on a single MRI to establish joint coordinate systems (6) and were applied to the other scans by again using the TrICP. Articular cartilage contact area was estimated for each compartment independently by first generating a 100 by 100 rectangular grid of the tibial cartilage along a plane estimating the surface of the tibial plateau. Each grid space was extruded to the surface of the cartilage and deemed to be in contact if it was within 0.5 mm of the nearest femoral cartilage. Cartilage surfaces were retraced after a period of two weeks had passed. Reported articular cartilage contact area estimates are an average of the two calculations. In order to account for

variations in joint size between subjects, the data were normalized to a tibial plateau surface area estimate. The model points that comprised the tibial plateau were input into a custom MATLAB (MathWorks, Natick, MA) routine that identified the anterior-posterior and medial-lateral lengths of the surface. Raw contact area data were normalized by dividing by the rectangular area generated and multiplying by 100 to estimate a percentage of the tibial plateau in contact.

4.2.4 Data analysis

Only data from the medial compartment were included in the analysis and the leg with the more severe medial KL grade was selected for analysis. If disease progression was equal in both medial compartments, we attempted to balance the number of left and right legs included in the analysis. Statistical analysis of the data was performed using SPSS 16.0 (SPSS Inc., Chicago, IL). Subject characteristics were compared using independent t-tests if the parametric assumptions of the test were met. The non-parametric equivalent was used if Levene's test found the data to have unequal variances. Contact area data and knee flexion angle were compared using two-tailed Pearson's product moment correlation analysis. P values ≤ 0.05 were considered significant.

4.3 Results

Data from 11 healthy controls and 11 OA subjects were analyzed in this study. A comparison of subject characteristics (Table 4.1) shows that significant differences were found only in group weight.

Table 4.1 Group characteristics (mean ± standard deviation)

	Healthy	OA
N	11	11
% Female	72.7	72.7
% Right Leg	63.6	63.6
Age (yrs)	55.4 ± 10.3	59.9 ± 9.1
Height (m)	1.66 ± 0.04	1.70 ± 0.09
Weight (kg)**	71.0 ± 8.1	85.6 ± 19.1
BMI (kg/m^2)	25.9 ± 3.6	29.5 ± 5.5

** $p \leq 0.05$

Healthy control subjects were found to have a significant ($p \leq 0.01$) correlation between medial compartment articular cartilage contact area and knee flexion angle, while the OA subjects did not ($p = 0.81$). After the data were normalized, the healthy control subjects were again found to have a significant ($p \leq 0.01$) correlation between articular cartilage contact area and knee flexion angle, while the OA subjects again did not ($p = 0.34$). The raw and normalized data can be seen in Figures 4.1 and 4.2, respectively. Linear regression analysis predicted medial compartment contact areas of 392.8, 335.3, and 277.8 mm^2 for the healthy controls at 0°, 15°, and 30° relative knee flexion, respectively. Similarly in the moderate OA subjects, medial compartment contact areas of 486.4, 478.0, and 469.5 were found (Table 4.2). In both the raw and normalized cases, the regression line predicted an increased articular cartilage contact area in the OA subjects.

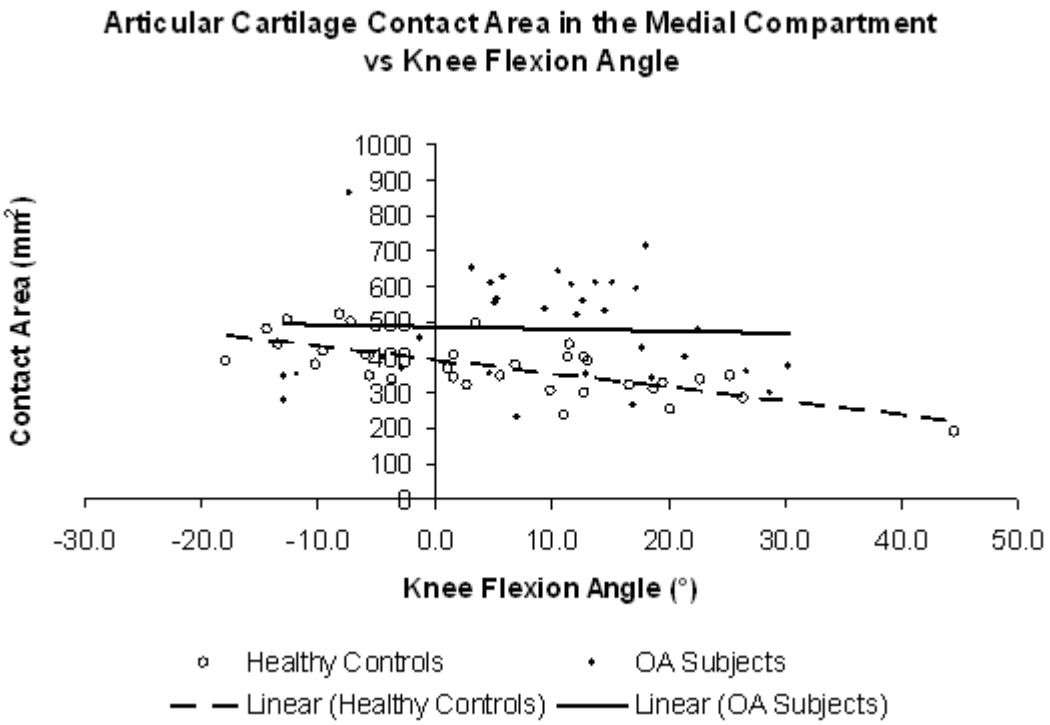

Figure 4.1 **Articular cartilage contact area in the medial compartment of the tibiofemoral joint plotted against knee flexion angle in moderate knee OA subjects and healthy controls with corresponding regression lines. The healthy controls were found to have a significant ($p \leq 0.01$) correlation between knee flexion angle and contact area, while the OA subjects did not ($p = 0.81$).**

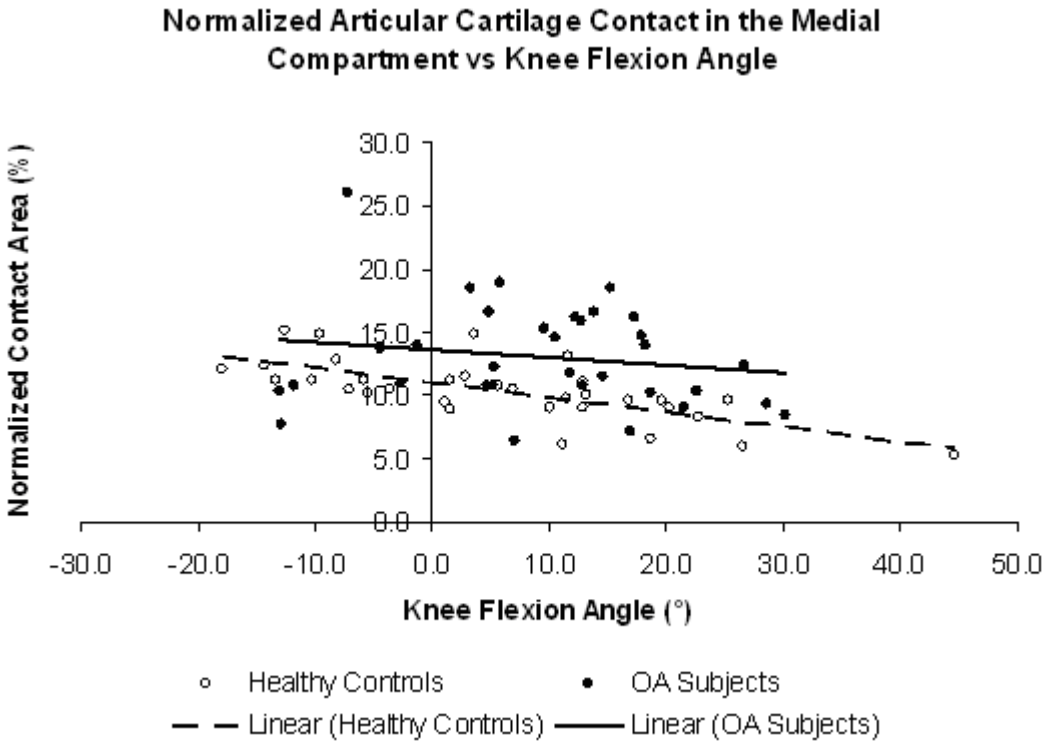

Figure 4.2 Normalized articular cartilage contact area in the medial compartment of the tibiofemoral joint in healthy controls and OA subjects. Healthy control subjects were found to have a significant ($p \leq 0.01$) correlation between knee flexion angle and contact area, while OA subjects did not ($p = 0.34$).

Table 4.2 Estimates of group articular cartilage contact area generated from linear regression lines. OA subjects were found to have higher mean articular cartilage contact areas across all knee flexion angles considered in both the raw and normalized data cases.

Knee Flexion Angle (°)	Raw Contact Area (mm^2)		Normalized Contact Area (%)	
	OA	Healthy Controls	OA	Healthy Controls
0	486.4	392.8	13.62	11.04
15	478.0	335.3	12.71	9.27
30	469.5	277.8	11.79	7.50

4.4 Discussion

Articular cartilage contact area in the tibiofemoral joint was successfully estimated in subjects with moderate knee OA and healthy controls. Although significant differences between the two groups were found in subject weight, it is not believed to have confounded the results. Increased weight has the potential to increase contact area due to the increased joint loading, however it is not believed to have any effect on the relationship with knee flexion.

In the healthy control subjects, medial compartment contact area decreased with increasing knee flexion. As the knee flexes, femoral geometry dictates decreased tibiofemoral articular cartilage contact area. Our results corroborate previous investigations of medial compartment tibiofemoral contact area both *in vitro* (8) and *in vivo* (7,10). In a study of 14 cadavers Kettelkamp and Jacobs (8) found approximate medial compartment articular cartilage contact areas of 480, 400, and 380 mm^2 at 0, 15, and 30° knee flexion, respectively. These contact area estimates are greater than estimates from our study by 87.2, 64.7, and 102.2 mm^2, respectively, however most of

the soft tissue including the menisci were removed prior to data collection, which may explain the increased articular cartilage contact area. Patel et al. (10) investigated articular cartilage contact area of the medial compartment using a MRI based method and incorporated pseudo-weightbearing of the foot (133 N) using a custom apparatus. Their contact area estimates of 374, 355, and 340 mm^2 at 0, 15, and 30° knee flexion are lower than our results; however this may be explained by the increased average load experienced by our subjects (246 N, assuming equal weight distribution). Hinterwimmer et al. (7) also used MRI to investigate articular cartilage contact area in healthy adults and generated medial compartment estimates of 487, 404, and 302 mm^2 at 0, 30, and 90° knee flexion in a cohort of 12 subjects. These results match well with the results from our study. Both Patel et al. (10) and Hinterwimmer et al. (7) identified articular cartilage contact area by manually identifying areas on MRI slices that appeared to be in contact and multiplying this length by the slice thickness to generate an area. Our method is an improvement over these previous methods because we were able to generate a three dimensional model that gives a more accurate estimate of cartilage contact area between image slices by incorporating previous MRI data into the modeling process and may explain some of the differences in results.

Articular cartilage contact area has not been studied in the knee OA population *in vivo*. The results of this study suggest that OA subjects undergo changes with regard to articular cartilage contact area through an approximate range of weightbearing flexion angles achieved during gait. The increased contact area seen in OA subjects may be due to increased cartilage compliance, meniscal extrusion, cartilage degradation, increased role in weightbearing, or any combination thereof. The regression lines predicted an increased cartilage contact area across all flexion

angles studied. If mechanical stress is believed to be a key component of OA progression, this would suggest that the increased contact area is a biomechanical adaptation to distribute load and limit the rate of progression. Using ½ body weight as an estimate of axial load, at full extension the moderate OA subjects were found to have an average normal stress of 0.62 MPa, while the healthy controls had an average normal stress of 0.57 MPa. It is noteworthy that OA stress was elevated relative to healthy age matched controls even with increased articular cartilage contact area.

There are several potential limitations that need to be considered when interpreting our results. First, we considered only articular cartilage on articular cartilage contact area. Bone on articular cartilage contact in the joint is unlikely because we excluded subjects with severe (KL = 4) OA. Meniscal-articular cartilage contact area was also excluded. There is disagreement in the literature as to the weightbearing function of the meniscus. Shefelbine et al. (13) has suggested that the meniscus has a substantial weightbearing function, while other investigators have suggested that its contribution is minimal or negligible (10,11). Our results ignore the loadbearing function of the meniscus, if present. Secondly, it was not possible to estimate the load transmitted through the medial compartment to directly evaluate the mechanical stress hypothesis. We instructed the subjects to equally distribute their weight between their legs during the data collection process, however we were unable to quantify weight distribution. Varus/valgus alignment was also not considered, which also likely influences the load transmitted through each of the tibiofemoral joints and therefore may affect the articular cartilage contact area of each compartment. Finally, although subjects were instructed to "stand as straight as possible", 16 of the 22 total subjects demonstrated some level of hyper-extension.

Patel et al. (10) chose to set full extension as 0° knee flexion possibly due to similar findings. Normalizing the data this way limits the external validity of the investigation.

4.5 Conclusions

The relationship between medial compartment tibiofemoral articular cartilage contact area and knee flexion was evaluated in subjects with moderate knee OA and healthy controls. The healthy controls were found to have a significant relationship between contact area and knee flexion in both the raw and normalized data sets, while the OA subjects were found to lack this relationship in both instances. The overall increase in articular cartilage contact area across these flexion angles suggests that it may be a biomechanical adaptation to decrease mechanical stress across the joint. Future studies will attempt to estimate joint contact forces to improve the understanding of the role that mechanical stress may play in progression of knee OA.

4.6 References

1. Barrance P, Pohl M, Noehren B, Barrios J, Davis I. Bone Surface Tracking for Standing Knee MRI: A Validation Study. *Proceedings of the 2007 American Society of Biomechanics Annual Conference*; 2007 Aug 22-25: Stanford (CA). Stanford University; 2007. p1-10.

2. Brandt KD, Dieppe P, Radin EL. Etiopathogenesis of Osteoarthritis. *Rheum Dis Clin North Am*. 2008;34(3):531-59.

3. Buckwalter JA, Saltzman C, Brown T. The Impact of Osteoarthritis: Implications for Research. *Clin Orthop Relat Res*. 2004;427S:S6-15.

4. Chetverikov D, Stepanov D, Krsek P. Robust euclidean alignment of 3D point sets: the trimmed iterative closest point algorithm. *Image Vis Comput*. 2005;23(3):299-309.

5. Fukubayashi T, Kurosawa H. The Contact Area and Pressure Distribution Pattern of the Knee: A Study of Normal and Osteoarthrotic Knee Joints. *Acta Orthop Scand*. 1980;51(6):871-9.

6. Grood ES, Suntay WJ. A Joint Coordinate System for the Clinical Description of Three-Dimensional Motions: Application to the Knee. *J Biomech Eng*. 1983;105(2):136-44.

7. Hinterwimmer S, Gotthardt M, von Eisenhart-Rothe R, Sauerland S, Siebert M, Vogl T, Eckstein F, Graichen H. In vivo contact areas of the knee in patients with patellar subluxation. *J Biomech*. 2005;38(10):2095-101.

8. Kettelkamp DB, Jacobs AW. Tibiofemoral Contact Area – Determination and Implications. *J Bone Joint Surg A*. 1972;54(2):349-56.

9. Miyazaki T, Wada M, Kawahara H, Sato M, Baba H, Shimada S. Dynamic load at baseline can predict radiographic disease progression in medial compartment knee osteoarthritis. *Ann Rheum Dis*. 2002;61(7):617-22.

10. Patel VV, Hall K, Ries M, Lotz J, Ozhinsky E, Lindsey C, Lu Y, Majumdar S. A three-dimensional MRI analysis of knee kinematics. *J Orthop Res*. 2004;22(2):283-92.

11. Périé D, Hobatho MC. In vivo determination of contact areas and pressure of the femorotibial joint using non-linear finite element analysis. *Clin Biomech*. 1998;13(6):394-402.

12. Raynauld JP, Martel-Pelletier J, Berthiaume MJ, Beaudoin G, Choquette D, Haraoui B, Tannenbaum H, Meyer JM, Beary JF, Cline GA, Pelletier JP. Long term evaluation of disease progression through the quantitative magnetic resonance imaging of symptomatic knee osteoarthritis patients: correlation with clinical symptoms and radiographic changes. *Arthritis Res Ther*. 2006;8(1):R21.

13. Shefelbine SJ, Ma CB, Lee KY, Schrumpf MA, Patel P, Safran MR, Slavinsky JP, Majumdar S. MRI Analysis of In Vivo Meniscal and Tibiofemoral Kinematics in ACL-Deficient and Normal Knees. *J Orthop Res*. 2006;24(6):1208-17.

14. Wluka AE, Stuckey S, Snaddon J, Cicuttini FM. The Determinants of Change in Tibial Cartilage Volume in Osteoarthritic Knees. *Arthritis Rheum*. 2002;46(8):2065-72.

15. Zhao D, Banks SA, Mitchell KH, D'Lima DD, Colwell CW Jr, Fregly BJ. Correlation between the Knee Adduction Torque and Medial Contact Force for a Variety of Gait Patterns. *J Orthop Res*. 2007;25(6):789-97.

Chapter 5

CONCLUSIONS AND FUTURE WORK

Tibiofemoral articular cartilage contact area was estimated using an existing MRI based modeling method. Confidence in the method was achieved through analysis of data from a single healthy subject. Data from this subject were compared to existing literature and analyzed using a series of assessments to further establish confidence in the method. In the second half of the study, the relationship between knee flexion and medial compartment articular cartilage contact area in subjects with moderate knee OA and healthy, age matched controls was investigated. The healthy controls were found to have decreasing contact area with increasing knee flexion ($p \leq 0.01$), similar to previous investigations. The moderate knee OA subjects were not found to have this same relationship. Linear regression analysis found that the moderate knee OA subjects had higher medial compartment articular cartilage contact area throughout the range of flexion angles studied. The knee flexion angles investigated are common during weightbearing in gait and may represent a biomechanical adaptation to decrease the magnitude of mechanical stress applied.

This was the first *in vivo* study to investigate articular cartilage contact area in subjects with knee OA. Differences between moderate OA subjects and healthy, age matched controls were found in their respective relationships between medial compartment articular cartilage contact area and knee flexion. This advocates for further investigation into articular cartilage contact area in subjects with knee OA.

Future work will involve recruitment and data collection on additional healthy and moderate OA subjects. Power analysis suggests that differences of medial compartment articular cartilage contact area will be seen with 17 subjects per group, with the OA subjects having greater contact area. Gait data is also available on subjects included in this study and efforts will be made to establish relationships between contact area and gait variables. FEA will be attempted through use of musculoskeletal simulations generated from the gait data and models of the knee generated from MRI in an effort to more quantitatively assess the role of mechanical stress in OA. FEA has the potential to quantify stress distribution within the articular cartilage contact area as well as identify of the locations of peak stress, which are both highly important in understanding the role that stress may play the role of progression. Follow-up MRI and gait data collections will also be performed 18-24 months after the baseline test. Ideally, baseline data will allow for identification of subjects at higher risk for progression of OA and will be validated through radiographic progression at the follow-up. Once risk factors for OA progression are identified, specific interventions can be generated.

REFERENCES

Allaire R, Muriuki M, Gilbertson L, Harner CD. Biomechanical Consequences of a Tear of the Posterior Root of the Medial Meniscus. Similar to Total Meniscectomy. *J Bone Joint Surg Am*. 2008;90(9):1922-31.

Altman R, Asch E, Bloch D, Bole G, Borenstein D, Brandt K, Christy W, Cooke TD, Greenwald R, Hochberg M, Howell D, Kaplan D, Koopman W, Longley S, Mankin H, McShane DJ, Medsger T, Meenan R, Mikkelsen W, Moskowitz R, Murphy W, Rothschild B, Segal M, Sokoloff L, Wolfe F. Development of criteria for the classification and reporting of osteoarthritis. *Arthritis Rheum*. 1986;29(8):1039-49.

American Academy of Orthopaedic Surgeons. Osteoarthritis of the Knee: Evidence-based Resources [Internet]. Rosemont (IL):American Academy of Orthopaedic Surgeons; 2004.

American Academy of Orthopaedic Surgeons. Osteoarthritis of the Knee: State of the Condition [Internet]. Rosemont (IL):American Academy of Orthopaedic Surgeons; 2004.

American Academy of Orthopaedic Surgeons. Osteoarthritis of the Knee: Treatment Options [Internet]. Rosemont (IL):American Academy of Orthopaedic Surgeons; 2004.

Amin S, LaValley MP, Guermazi A, Grigoryan M, Hunter DJ, Clancy M, Niu JB, Gale DR, Felson DT. The Relationship Between Cartilage Loss on magnetic Resonance Imaging and Radiographic Progression in Men and Women with Knee Osteoarthritis. *Arthritis Rheum*. 2005;52(10):3152-9.

Andriacchi TP, Mundermann A, Smith RL, Alexander EJ, Dyrby CO, Koo S. A Framework for the in Vivo Pathomechanics of Osteoarthritis at the Knee. *Ann Biomed Eng*. 2004;32(3):447-57.

Arokoski JP, Jurvelin JS, Väätäinen U, Helminen HJ. Normal and pathological adaptations of articular cartilage to joint loading. *Scand J Med Sci Sports*. 2000;10(4):183-5.

Asano T, Akagi M, Tanaka K, Tamura J, Nakamura T. In Vivo Three-Dimensional Knee Kinematics Using a Biplanar Image-Matching Technique. *Clin Orthop Relat Res*. 2001;388:157-66.

Barrance P, Pohl M, Noehren B, Barrios J, Davis I. Bone Surface Tracking for Standing Knee MRI: A Validation Study. *Proceedings of the 2007 American Society of Biomechanics Annual Conference*; 2007 Aug 22-25: Stanford (CA). Stanford University; 2007. p1-10.

Bei Y, Fregly B. Multibody dynamic simulation of knee contact mechanics. *Med Eng Phys*. 2004;26(9):777-89.

Berthiaume MJ, Raynauld JP, Martel-Pelletier J, Labonte F, Beaudoin G, Bloch DA, Choquette D, Haraoui B, Altman RD, Hochberg M, Meyer JM, Cline GA, Pelletier JP. Meniscal tear and extrusion are strongly associated with progression of symptomatic knee osteoarthritis as assessed by quantitative magnetic resonance imaging. *Ann Rheum Dis*. 2005;64(4):556-63.

Besier TF, Draper CE, Gold GE, Beaupré GS, Delp SL. Patellofemoral joint contact area increases with knee flexion and weight-bearing. *J Orthop Res*. 2005;23:345-50.

Bingham JT, Papannagari R, Van de Velde SK, Gross C, Gill TJ, Felson DT, Rubash HE, Li G. In vivo cartilage contact deformation in the healthy human tibiofemoral joint. *Rheumatology (Oxford)*. 2008;47:1622-7.

Brandt KD, Dieppe P, Radin EL. Etiopathogenesis of Osteoarthritis. *Rheum Dis Clin North Am*. 2008;34:531-59.

Buckwalter JA, Saltzman C, Brown T. The Impact of Osteoarthritis: Implications for Research. *Clin Orthop Relat Res*. 2004;427S: S6-15.

Chetverikov D, Stepanov D, Krsek P. Robust euclidean alignment of 3D point sets: the trimmed iterative closest point algorithm. *Image Vis Comput*. 2005;23(3):299-309.

Cicuttini F, Hankin J, Jones G, Wluka A. Comparison of conventional standing knee radiographs and magnetic resonance imaging in assessing progression of tibiofemoral joint osteoarthritis. *Osteoarthritis Cartilage*. 2005;13(8):722-7.

Cooper C, Snow S, McAlindon TE, Kellingray S, Stuart B, Coggon D, Dieppe PA. Risk Factors for the Incidence and Progression of Radiographic Knee Osteoarthritis. *Arthritis Rheum*. 2000;43(5):995-1000.

DeFrate LE, Sun H, Gill TJ, Rubash HE, Li G. In vivo tibiofemoral contact analysis using 3D MRI-based knee models. *J Biomech*. 2004;37(10):1499-504.

Donahue TL, Hull ML, Rashid MM, Jacobs CR. A Finite Element Model of the Human Knee Joint for the Study of Tibio-Femoral Contact. *J Biomech Eng*. 2002;124(3):273-80.

Eckstein F, Glaser C. Measuring Cartilage Morphology with Quantitative Magnetic Resonance Imaging. *Semin Musculoskelet Radiol*. 2004;8(4):329-53.

Federico S, La Rosa G, Herzog W, Wu JZ. Effect of Fluid Boundary Conditions on Joint Contact Mechanics and Applications to the Modeling of Osteoarthritic Joints. *J Biomech Eng*. 2004;126:220-5.

Felson DT, Zhang YQ. An Update on the Epidemiology of Knee and Hip Osteoarthritis with a View to Prevention. *Arthritis Rheum*. 1998;41(8):1343-55.

Felson. DT. Developments in the clinical understanding of osteoarthritis. *Arthritis Res Ther*. 2009;11(1):203.

Fukubayashi T, Kurosawa H. The Contact Area and Pressure Distribution Pattern of the Knee: A Study of Normal and Osteoarthrotic Knee Joints. *Acta Orthop Scand*. 1980;51(6):871-9.

Gandy SJ, Dieppe PA, Keen MC, Maciewicz RA, Watt I, Waterton JC. No loss of cartilage volume over three years in patients with knee osteoarthritis as assessed by magnetic resonance imaging. *Osteoarthritis Cartilage*. 2002;10(12):929-37.

Gold GE, Beaulieu CF. Future of MR Imaging of Articular Cartilage. *Semin Musculoskelet Radiol*. 2001;5(4):313-27.

Gold GE, Besier TF, Draper CE, Asakawa DS, Delp SL, Beaupre GS. Weight-Bearing MRI of Patellofemoral Joint Cartilage Contact Area. *J Magn Reson Imaging*. 2004;20(3):526-30.

Grood ES, Suntay WJ. A Joint Coordinate System for the Clinical Description of Three-Dimensional Motions: Application to the Knee. *J Biomech Eng*. 1983;105(2):136-44.

Hamilton N, Luttgens K. *Kinesiology: Scientific Basis of Human Motion*. 10th ed. New York (NY): McGraw-Hill; 2002. p. 183-93.

Hill PF, Vedi V, Williams A, Iwaki H, Pinskerova V, Freeman MA. Tibiofemoral movement 2: the loaded and unloaded living knee studied by MRI. *J Bone Joint Surg Br*. 2000;82(8):1196-8.

Hinterwimmer S, Gotthardt M, von Eisenhart-Rothe R, Sauerland S, Siebert M, Vogl T, Eckstein F, Graichen H. In vivo contact areas of the knee in patients with patellar subluxation. *J Biomech*. 2005;38(10):2095-101.

Hunter DJ, Niu JB, Felson DT, Harvey WF, Gross KD, McCree P, Aliabadi P, Sack B, Zhang YQ. Knee Alignment Does Not Predict Incident Osteoarthritis - The Framingham Osteoarthritis Study. *Arthritis Rheum*. 2007;56(4):1212-18.

Kellgren JH, Lawrence JS. Radiological assessment of osteo-arthritis. *Ann Rheum Dis*. 1957;16:494-502.

Kettelkamp DB, Jacobs AW. Tibiofemoral Contact Area – Determination and Implications. *J Bone Joint Surg A*. 1972;54(2):349-56.

Lee SJ, Aadalen KJ, Malaviya P, Lorenz EP, Hayden JK, Farr J, Kang RW, Cole BJ. Tibiofemoral Contact Mechanics After Serial Medial Meniscectomies in the Human Cadaveric Knee. *Am J Sports Med*. 2006;34(8):1334-44.

Li G, DeFrate LE, Park SE, Gill TJ, Rubash HE. In Vivo Articular Cartilage Contact Kinematics of the Knee: An Investigation Using Dual-Orthogonal Fluoroscopy and Magnetic Resonance Image-Based Computer Model. *Am J Sports Med*. 2005;33(1):102-7.

Martel-Pelletier J, Boileau C, Pelletier JP, Roughley PJ. Cartilage in normal and osteoarthritis conditions. *Best Pract Res Clin Rheumatol*. 2008;22(2):351-84.

Miyazaki T, Wada M, Kawahara H, Sato M, Baba H, Shimada S. Dynamic load at baseline can predict radiographic disease progression in medial compartment knee osteoarthritis. *Ann Rheum Dis*. 2002;61(7):617-22.

Moro-oka TA, Hamai S, Miura H, Shimoto T, Higaki H, Fregly BJ, Iwamoto Y, Banks SA. Dynamic Activity Dependence of In Vivo Normal Knee Kinematics. *J Orthop Res*. 2008;26(4):428-34.

Niu J, Zhang YQ, Torner J, Nevitt M, Lewis CE, Aliabadi P, Sack B, Clancy M, Sharma L, Felson DT. Is Obesity a Risk Factor for Progressive Radiographic Knee Osteoarthritis? *Arthritis Care Res*. 2009;61(3):329-35.

North Carolina School of Science and Mathematics [Internet]. Durham, NC. Experience NCSSM; [cited 2009 Nov 3]. Available from: http://www.ncssm.edu/library/dirt/Valerie%20Todd/Basic%20Anatomy.html

Patel VV, Hall K, Ries M, Lotz J, Ozhinsky E, Lindsey C, Lu Y, Majumdar S. A three-dimensional MRI analysis of knee kinematics. *J Orthop Res*. 2004;22(2):283-92.

Pelletier JP, Raynauld JP, Berthiaume MJ, Abram F, Choquette D, Haraoui B, Beary JF, Cline GA, Meyer JM, Martel-Pelletier J. Risk factors associated with the loss of cartilage volume on weight-bearing areas in knee osteoarthritis patients assessed by quantitative magnetic resonance imaging: a longitudinal study. *Arthritis Res Ther*. 2007;9(4):R74.

Périé D, Hobatho MC. In vivo determination of contact areas and pressure of the femorotibial joint using non-linear finite element analysis. *Clin Biomech*. 1998;13(6):394-402.

Potter HG, Foo LF. Magnetic Resonance Imaging of Articular Cartilage: Trauma, Degeneration, and Repair. *Am J Sports Med*. 2006;34(4):661-77.

Raynauld JP, Kauffmann C, Beaudoin G, Berthiaume MJ, de Guise JA, Bloch DA, Camacho F, Godbout B, Altman RD, Hochberg M, Meyer JM, Cline G, Pelletier JP, Martel-Pelletier J. Reliability of a quantification imaging system using magnetic resonance images to measure cartilage thickness and volume in human normal and osteoarthritic knees. *Osteoarthritis Cartilage*. 2003;11(5):351-60.

Raynauld JP, Martel-Pelletier J, Berthiaume MJ, Beaudoin G, Choquette D, Haraoui B, Tannenbaum H, Meyer JM, Beary JF, Cline GA, Pelletier JP. Long term evaluation of disease progression through the quantitative magnetic resonance imaging of symptomatic knee osteoarthritis patients: correlation with clinical symptoms and radiographic changes. *Arthritis Res Ther*. 2006;8(1):R21.

Recht M, Bobic V, Burstein D, Disler D, Gold G, Gray M, Kramer J, Lang P, McCauley T, Winalski C. Magnetic Resonance Imaging of Articular Cartilage. *Clin Orthop Relat Res*. 2001;391:S379-96.

Shefelbine SJ, Ma CB, Lee KY, Schrumpf MA, Patel P, Safran MR, Slavinsky JP, Majumdar S. MRI Analysis of In Vivo Meniscal and Tibiofemoral Kinematics in ACL-Deficient and Normal Knees. *J Orthop Res*. 2006;24(6):1208-17.

Stammberger T, Eckstein F, Englmeier KH, Reiser M. Determination of 3D Cartilage Thickness Data From MR Imaging: Computational Method and Reproducibility in the Living. *Magn Reson Med*. 1999;41(3):529-36.

Wluka AE, Stuckey S, Snaddon J, Cicuttini FM. The Determinants of Change in Tibial Cartilage Volume in Osteoarthritic Knees. *Arthritis Rheum*. 2002;46(8):2065-72.

Wretenberg P, Ramsey DK, Németh G. Tibiofemoral contact points relative to flexion angle measured with MRI. *Clin Biomech*. 2002;17(6):477-85.

Wu JZ, Herzog W, Epstein M. Joint contact mechanics in the early stages of osteoarthritis. *Med Eng Phys*. 2000;22(1):1-12.

Zhao D, Banks SA, Mitchell KH, D'Lima DD, Colwell CW Jr, Fregly BJ. Correlation between the Knee Adduction Torque and Medial Contact Force for a Variety of Gait Patterns. *J Orthop Res*. 2007;25(6):789-97.